EvaporaSun

PASSIVE EVAPORATIVE COOLING SYSTEM FOR PHOTOVOLTAICS

MEAM Senior Design (MEAM 445/446)
Final Report
September 2015 – May 2016
May 2nd, 2016

Department of Mechanical Engineering and Applied Mechanics

Faculty Advisor: Dr. Portonovo Ayyaswamy | *Asa Whitney Professor of Dynamical Engineering*
ayya@seas.upenn.edu
Instructor: Dr. Graham Wabiszewski | *Lecturer of Mechanical Engineering*
grahamw@seas.upenn.edu

Team Members:

Romer Beato *beator@seas.upenn.edu*
Jeremy Santiago *sajeremy@seas.upenn.edu*
Qizhan Tam *tqizhan@seas.upenn.edu*
Saagarika Thanvi *sthanvi@seas.upenn.edu*
TEAM TRANSLUSUN (08)

ABSTRACT

Team TransluSun is increasing the power output of solar photovoltaic panels using the EvaporaSun (EVA) system. With climate change being an ever-pressing issue, photovoltaics can help mitigate carbon emissions. However, their power output and lifetime degrade under high operating temperatures, common to areas with the highest solar energy potential. The existing solution is to spray water onto a solar panel's surface. This not only consumes power through pumps and electronics, but also causes mineral deposits on the solar panel's surface. Eva is a fully passive system that cools solar panels without the deficiencies of the existing solution. It works by using a cotton wick to transport water through capillary action from a reservoir to the back of the solar panel. The reservoir's water level is maintained by a float valve. The Eva system is cost effective, reliable and does not consume energy during its operation.

Investigations were carried out on the performance of different wicking materials, the effect of system parameters on wicking rate and evaporative cooling. The experiments were performed using heat sheets to simulate solar radiation, thermocouples to measure temperature change and testing rigs to hold the solar panel at varying angles. Eva managed to reduce solar panel temperature under simulated moderate solar irradiation (900W/m^2) by 15^{o}C, effectively increasing power output by 7.5%. Future work includes studying other synthetic materials to increase the wick's lifespan and system capabilities.

Team TransluSun is comprised of Romer Beato, Jeremy Santiago, Qizhan Tam, and Saagarika Thanvi and advised by Professor Portonovo Ayyaswamy

TABLE OF CONTENTS

SECTION 1: ***EXECUTIVE SUMMARY***

Solar photovoltaic panels have been an increasingly utilized technology in the efforts of mitigating climate change. While module prices of have been decreasing and cell efficiencies have been increasing, high temperatures still decrease the power output of solar panels. Solar panels perform best in areas with high solar irradiation which is consequently often areas with high ambient temperatures. For every degree Celsius the solar panel is above 25 degrees Celsius, the panel loses 0.45% of its rated power output which can result in 25% power loss for a panel at 80 degrees Celsius. The EvaporaSun system (Eva) was created to address the problem of solar panel power losses in high temperatures conditions by developing a low cost cooling system.

During the fall semester, different cooling methods were studied in order to decide the most cost effective cooling system. Evaporative cooling, heat fin cooling, and heat exchanger cooling were the three cooling methods studied and compared in order to determine the most cost effective cooling method. A 5 W solar panel was heated to a steady state temperature of 50 degrees Celsius in an insulated box and cooled along the backs side of the panel with different cooling methods. Based on the temperature difference achieved in experiments and on projected costs to implement different cooling systems for large scale panels, evaporative cooling was found to be the most effective cooling method of the three tested.

During the beginning of the spring semester, the evaporative cooling method was further studied in order to optimize energy usage of the system and power gained from the use of the system. In the evaporative cooling method category, water spray cooling and cotton wick cooling were considered cooling mechanisms. It was found that cotton wick cooling had the greatest potential because it did not require the utilization of electronics or pumps to transport water along the back surface of the panel and it had a comparable panel temperature decrease of 20 degrees Celsius.

With the cotton wick cooling method decided upon, prototyping and further experiments began in February and March to justify design choices of the Eva system. The wicking characteristics of cotton, ribbed cotton, polyester, and cotton-polyester mixes were first compared with each other by different standards. The main quantity measured to compare materials was the amount of time it took to transport water through the wicking material, known as the wicking rate. The wicking rate was measured against parameters of uptake height (the vertical height water travels before being transported through downward orientation), orientation of water traveling up, down, or at an inclined angle, and the tensile force applied to stretch the material. The main findings from the wicking experiments were that: 1) uptake height can be used to adjust the wicking rate of the material, 2) wicking rate increases when traveling downwards through material, and 3) wicking rate decreases with applied tensile forces. It was also found that ribbed cotton performed the best out of the compared wicking materials because it had the fastest wicking rate which can be controlled with varying uptake heights.

The results from the wicking experiments were used to lead the design of small scale prototype which was used to both test the functionality of the system and used as an apparatus for evaporation rate experiments. The design criteria for the Eva system was based on making it low cost and low energy consuming. One of the first mechanisms considered for the Eva system prototype was the process for storing and transporting water. Among various devices including electronic sensors and different mechanical valves, a float valve was implemented because of its low cost and it ability to function without the use of energy. The float valve is attached inside a container known

as the Wick Containment Unit (WCU) that houses both the water and cotton wick for the system. The WCU is attached on the top back side of an inclined solar panel where the potential wicking rate is greatest. The cotton cannot be stretched across the panel because it would reduce the potential wicking rate so a mesh is applied to the back to press the cotton to the back surface.

With the prototype constructed, evaporation rate experiments were conducted to calculate the water consumption that occurs when using the system. The water consumption completes the associated costs of a system to prove that the energy and money spent on water consumption is comparatively less than the energy gained from using the system. This finding is then further tested with simulations in an ideal location of Tallahassee, Florida with adequate water resources and solar irradiation to project cost savings with measured evaporation rates.

The EVA system was then scaled up to a 100W solar panel to validate the functionality in outdoor environments and to test the assumption that results from smaller scale experiments can be scaled to larger systems. It was found that the EVA system for a 100 W solar panel was able to achieve a temperature difference of 10°C in outdoor conditions in Philadelphia, PA with ambient temperatures reaching 22°C. The change in temperature acquired would correspond to saving the solar panel from a 4.5% power loss. The EVA system proved to be successful in lowering panel temperature and establishing cost savings.

Further considerations to improve the system include an in depth study on different weave patterns for wicking materials, a lifetime durability study of the product materials (particularly the pipe and wicking fabric used), power output measurements of the solar panel, and study of implementation of system to retrofit onto panels.

SECTION 2:

STATEMENT of ROLES and EXTERNAL CONTRIBUTIONS

TEAM MEMBERS

Romer Beato | beator@seas.upenn.edu
Responsible for creating the lamp setup for the indoor small scale testing, aiding in indoor tests of panels and wicking, aided in the design of medium scale EVA system, and ran field test of medium scale system.

Jeremy Santiago | sajeremy@seas.upenn.edu
Expertise in computer aided design, rapid prototyping, and project planning.
Responsible for creating heat exchanger experiment, completing study of water collector application, and designing and constructing medium scale EVA system.

Qizhan Tam | tqizhan@seas.upenn.edu
Expertise in experimentation, heat transfer, MATLAB, Arduino microcontrollers and electronics.
Responsible for investigating evaporative cooling on solar panels. Performed tests to model the wicking rate of fabric, heating and cooling tests to model the prototype system. Set up the electronics and fixtures for the small solar panels for testing and demonstration purposes.

Saagarika Thanvi | sthanvi@seas.upenn.edu
Fall semester project tasks included exploring the heat fin method of cooling for solar panels.
Spring semester project tasks included creating the small scale prototype of the EVA system and running simulations for the cost analysis of the entire system.

ADVISORS

Faculty

PORTONOVO AYYASWAMY, ASA WHITNEY PROFESSOR OF DYNAMICAL ENGINEERING

Dr. Ayyaswamy signed off on any necessary paperwork and overlooked the progress of the project.

Technical

IGOR BARGATIN, CLASS of 1965 TERM ASSISTANT PROFESSOR of MECHANICAL ENGINEERING and APPLIED MECHANICS

Dr. Bargatin provided the initial idea for this project. In addition, he advised the team about the wicking process and answered any general technical questions related to the testing and modeling of the cooling system.

MARK NIELSON, VICE PRESIDENT of STAFF SERVICES at DELAWARE ELECTRIC COOPERATIVE
Mr. Nielson provided data from the Bruce A. Memorial Solar Farm in Delaware that was used to create some of the models in the project.

JOSEPH VALDEZ, JOURNEYMAN MACHINIST at UNIVERSITY of PENNSYLVANIA
Mr. Valdez provided a lot of support related to the manufacturing of both the small scale and large scale version of the EVA system.

PETER SZCZENIAK, MANAGER, MANUFACTURING and FABRICATION SERVICES at UNIVERSITY of PENNSYLVANIA
Mr. Szczeniak provided advice related to the waterproofing of the small scale prototype of the Wick Containment Unit (WCU) of the EVA system.

RYAN QUIRK, INSTRUCTIONALLABORATORY COORDINATIOR at UNVIERSITY of PENNSYLVANIA
Mr. Quirk helped in 3D printing of parts.

GRAHAM WABISZEWSKI, Lecturer of MECHANICAL ENGINEERING and APPLIED MECHANICS at UNIVERSITY of PENNSYLVANIA

Dr. Wabiszewski provided us with valuable advice throughout the project to meet specific goals for a complete project.

SECTION 3:

BACKGROUND

Solar energy has become one of the most important renewable resources to pursue in recent efforts to cut down on carbon dioxide emissions due to the use of fossil fuels. It is an abundant and sustainable resource, and the world over is investing more in harvesting this energy source. To drive down carbon dioxide emissions with respect to a change in 2 degrees C, there needs to be an increase in solar energy production from 20 GW to 400 GW in the US alone, a twenty-fold increase which would provide enough power for 80 million homes [1].

Solar technology, and particularly solar photovoltaic (PV) panels, has been rapidly developing each year with the prices of these modules dropping and the efficiency of the systems increasing over time. Even with this increasing efficiency however, there are still factors that prevent these PV cells from reaching its maximum power output [2]. Some of the causes of reductions in power output are high temperatures (whose effects will be explained shortly), and stochastic factors like dust, leaves, or snow that block the surface of the panels thus preventing the panels from absorbing the full potential of the solar irradiance they receive [3].

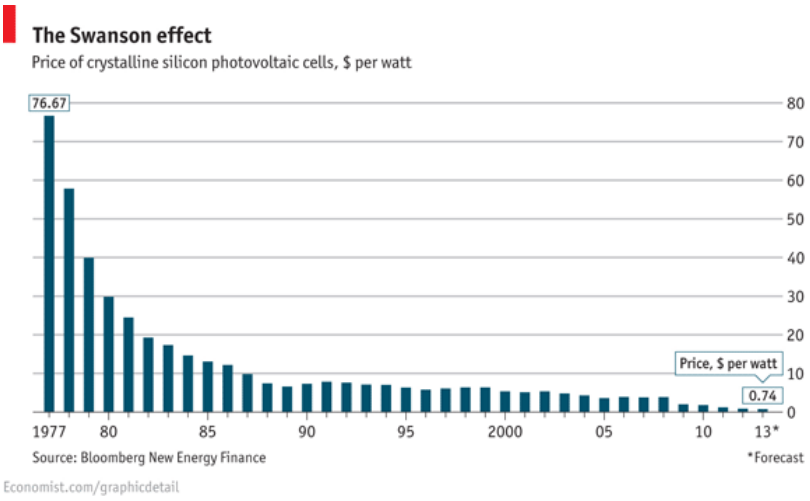

Figure 3.1: Swanson Effect.

In response to these factors there has been the adoption of systems to augment solar installations beginning in the early 2000's, like panel cleaners to clean sand off of surfaces in desert areas. [4] What enabled the adoption of these products that augment solar energy production is due the rapidly sinking costs of solar panels. As figure 3.1 shows costs for PV Cells have decreased by over 95% [5].

The factor reducing power output was found to be most pressing was the effect that temperature has on solar panels. High panel temperatures reduce the power output of solar panels with each degree in temperature increase above usual operating conditions, which is 25 C. In the beginning stages of the project information was gathered at the Bruce A. Henry Solar Farm owned by the Delaware Electric Cooperative, which uses the IM72 polycrystalline silicon panels from Motech. Those panels have a temperature coefficient of -0.46 +/- 0.02 %/°C [6]. This value represents the drop in maximum power per degree above 25°C [7]. In locations like Tucson Arizona, the

temperatures of these panels can reach up to 85°C. In Delaware, temperatures of the panel can reach easily over 50 °C, as shown in figure 3.2. At 50°C power output would be about 11-12% less than at 25°C, and a power loss of up to 20-25% in warm climate locations that increase panel temperatures to over 80 C. In addition to reducing the maximum power output of these solar cells, high temperatures also cause the panels to prematurely age and the rate of aging doubling every time there is an increase of 18 °C [2]. The hot temperatures can cause permanent structural damage due to the thermal stresses created by prolonged overheating [8].There are a few physical phenomena that underlie the increase in temperature, which then reduces the power output. The physics behind the power output drop of the solar panels starts with the efficiency of a panel to absorb photons. Below a certain energy level (which corresponds to a particular wavelength), the silicon will simply allow a photon to pass through unaffected. At a particular energy level known as the bandgap energy level (around 1.1 eV for most silicon cells), the panel absorbs the photon. This leads to the creation of an electron-hole pair. For energy levels higher than the bandgap energy, the panel absorbs the photon but the energy above 1.1 eV is considered excess. So if a photon with 1.6 eV is absorbed, 0.5 eV is considered excess. The excess energy is absorbed as heat by the silicon, which has two effects: it increases the temperature of the silicon, and that causes thermal emissions of photons, that could otherwise go to producing electricity.

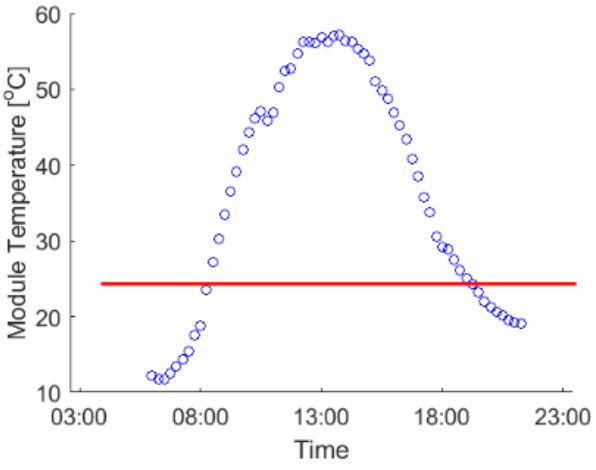

Figure 3.2: Daily temperature data of a solar panel (in blue) and a 25ºC marker (in red).

The power loss and life degradation of solar panels in high temperature conditions is a pressing issue that must be addressed. Even though there is this opportunity and need, there are no commercial solutions for dealing with cooling of solar panels on the residential, commercial, or utility scale. Nonetheless, there have been several research and design approaches that have been implemented in an attempt to lower the loss of power output. There are both passive and active cooling methods applied to solar panels. Passive relates to the use of natural environmental or mechanical structures to cool the panel without the need for any electro-mechanical systems. Active cooling is related to the use of some kind of electrical system to control the operation of the cooling mechanism.

There is an automated solar cleaner/cooler system that a company in South Korea called Integra Global. Their product, “Solmaks”, works as both a cleaner and cooler of the solar panels through using a water spray system. [9] Solmaks is shown in figure 3.3. When dust, snow, or any sort of debris obstruct the panel, a water spray system and brush is used to wipe clean the surface of the panels. In addition to this cleaning process, the water spray system operates at set intervals during the day to cool the panels. Solmaks consists of a station that houses the cleaning and cooling head

and its operating arms. This structure is attached to the top of the solar panel. These heads move along rails that are above the solar panel surface [9].

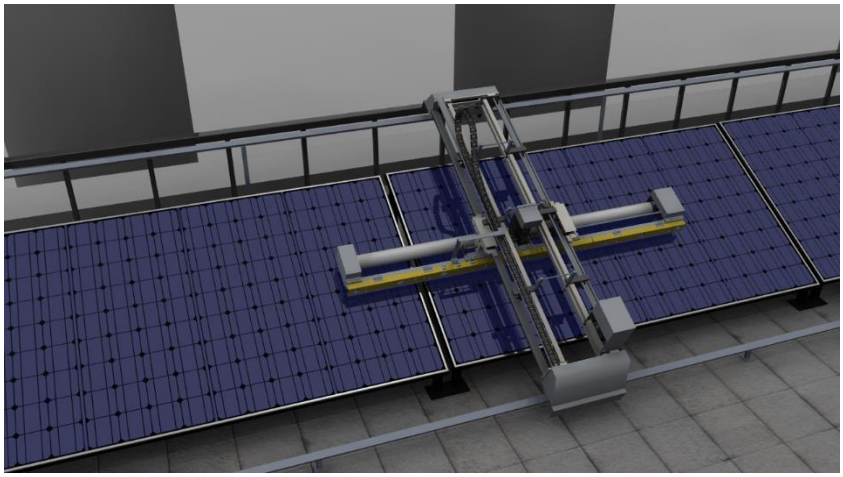

Figure 3.3: Solmaks cleaning and cooling system.

Solmaks could both clean and cool the solar photovoltaic modules, but is too large of a system for a single purpose. The amount of power needed to operate this system would substantially decrease the benefit of the power production from either cleaning or cooling panels on a larger scale.

Alongside the nascent development of commercial products, there has been research to create inexpensive passive methods for cooling [2]. Stanford researchers have used material science approach to cooling these cells by making an inexpensive coating of silica glass that lets the same amount of sunlight to be absorbed by the solar cells, reflecting away unabsorbed wavelengths for silicon, and enhancing the thermal radiation of silicon to cool panels faster [2]. This would reduce the need for another other method used to cool panels [2]. This coating has only been created on a lab scale however so if this could make a large impact of the solar energy market remains to be seen [2].

The cost of electricity around the world is usually much higher than in the US, where the average cost is $0.11 per kWh. This cost means that a system that cools panels will have a much higher profits in countries where cost of electricity is higher [10]. Alongside that though, the cost of electricity is stated to rise in the US, given the adoption of renewable energy sources and the changes in the process of electricity distribution [11]. Therefore, it will be important to improve the power output of these panels to outweigh the additional cost of electricity to run whatever system cools the panels.

SECTION 4:
OBJECTIVES

The purpose of this project was to develop a profitable apparatus that can decrease the high operating temperatures of the PV modules while operating at a commercial or utility scale. Profitability and energy usage is at the core of the project since that has been the limiting factor of intentions to tackle the problem of panel temperatures in the past. There is an important correlation with all of the desired metrics as well, a correlation that allowed a straightforward creation goals. The higher the temperature change, the more energy we save, the more money we save, and the more expensive our system can be. The creation of a high enough of a temperature change so as to make the system profitable was the goal, not necessarily the effort to reach particular numbers.

Goals

Basic (Energy)	**Intermediate (Economics)**	**Reach (Installation)**
Net energy increase.	Breakeven within 5 years.	Retrofits to existing solar panels.
System power usage < 0.155kWh/day	Total cost of system < $100	Modular design.
		Easy to install (<1 hr)

Table 4.1: Goals and objectives of the project.

To the left is the chart that described the project goals relating to energy use, economics, and installation. As mentioned earlier, the numbers for energy usage, cost of the system, and amount of time it would take for customers to break even are inseparable. The basic goals were related to the energy usage and automation of the system. As solar farms consist of tens of thousands of solar panels, the cooling system will have to be automated to avoid substantial labor costs.

Having a net energy increase is the most basic of goals for a system like this. The very premise of the project is rooted in improving the available energy to use. The usage of 0.155 kWh per day was based upon the maximum amount of cooling and power saved gained from a simulation that will be referenced later. At the outset this was a very optimistic goal, but it was foreseen that the balance between the system cost and profit from energy savings would easily be balanced by improving system design. The intermediate goals involved the economics side of the system. It was determined that a $100 system was the threshold for the solar panel to breakeven within 10 years of installation, which is equivalent to half of a solar panel's lifespan. This left time for the cooling system to profit and also to account for potential maintenance costs.

One of the other goals under considerations included installation. The goal was to create to improve the design of solar panel installation so that panels could be easily installed within an hour. Based on our exploration of the need for installation method improvements in the solar industry for field deployment this goal was dropped. Solar panel mounts come in a variety of shapes and sizes, and installation would depend on both the size of the panels and the mounting they're on. Attempting to improve and streamline panel mounting is a problem that even the industry is having trouble solving. So the last column regarding reach goals was out of reach from the very beginning of the project - it would require an entire project on its own.

SECTION 5:
DESIGN and REALIZATION

Cooling Methods

To make the most profit, the choice of cooling method was critical. Analysis of different cooling methods was done to figure out one would bring the most profit for the users of the proposed system. The three methods considered to help increase the power output of solar panels were: evaporative cooling through using a spray system, passive cooling through using heat fins, and a heat exchanger cooling system.

There were two main methods of cooling: active and passive cooling. Active cooling refers to the use of an electrical source to power the cooling method. On the other hand, passive cooling refers to cooling through the use of mechanical systems or through natural means. Initially, three forms of cooling methods were explored to see which one would be the most cost effective.

5.1 Evaporative Cooling for a Solar Panel in a Solar Farm

A thermal model of a solar panel installation is created to estimate, on average, the rate of water, m_{water}, that is required to keep a solar panel at a given temperature, T_{module}.

Solar irradiance power gain:

$$\dot{Q}_{gain,sun} = A_{solar} * \tau * \alpha * I_{sun}$$

τ = Transmissivity of glass

α = Absorptivity of solar panel

A_{solar} = Area of solar panel exposed to direct sunlight

I_{sun} = Solar irradiance.

Electricity generation power loss:

$$\dot{Q}_{loss,\ elec} = \eta * A_{solar} * \tau * \alpha * I_{sun}$$

$$\eta = \eta_0 *(1\text{-}k_T*(T_{module} - 25))$$

η = Efficiency of solar panel.

η_0 = Efficiency of solar panel at Standard Testing Conditions.

k_T = Temperature coefficient of solar panel.

Radiative rate of heat loss:

$$\dot{Q}_r = \mathcal{E} * \sigma * A_{free} * \left({T_{module}}^4 - {T_{ambient}}^4\right)$$

$\mathcal{E}$ = emissivity/absorptivity of solar panels (assume that solar panels are black bodies ε = 1)

A_{free} = "Free", or exposed surface area of panel available for the respective heat transfer processes to occur.

T_{module} = Solar panel module temperature.

$T_{ambient}$ = Ambient temperature.

Conductive rate of heat loss:

$$\dot{Q}_r = h_k * A_{free} * (T_{module} - T_{fixture})$$

$$h_k = \frac{A_{fixture}}{A_{free}} * \frac{k}{t}$$

Assuming that fixture's contact surface area << solar panel surface area

k = conductivity of fixture material,

t = thickness of solar panel fixtures,

$T_{fixture}$ = temperature of fixture ends.

Convective rate of heat loss:

$$\dot{Q}_c = h_c * A_{free} * (T_{module} - T_{ambient})$$

h_c = heat convection coefficient of solar panel surface

Rate of increase in heat stored in solar panel:

$$c_{panel} * m_{panel} = \Sigma(c_{material} * m_{material})$$

$$\dot{Q}_{stored} = c_{panel} * m_{panel} * (T_{module} - T_{module,pre})/t_{step} \qquad \text{Equation 5.1}$$

c_{panel} = Panel material's specific heat capacity

m_{panel} =Mass of solar panel.

$T_{module,pre}$ = Module temperature at the previous time-step.

Rate of heat loss from water evaporation:

$$\dot{Q}_{loss,\ water} = m_{water} * c_{water}/t_{step}$$

c_{water} = Water's latent heat of vaporization

m_{water} = Mass of water evaporated during each time-step.

t_{step} = Time between each change in temperatures.

Total rate of heat loss through natural means:

$$\dot{Q}_{loss,\ natural} = h_c * A_{free} * (T_{module} - T_{ambient}) + h_k * A_{free} * (T_{module} - T_{ambient}) + Q_r + \dot{Q}_{loss,\ water}$$

$\dot{Q}_{gain,sun}, \dot{Q}_{loss,\ elec}\ and\ \dot{Q}_{loss,\ natural}$ had to be recalculated for every t_{step} to **find the current module temperature T_{module}.** For simulation purposes, due to the assumption that conditions during t_{step} remain the same as the beginning of t_{step}, T_{module} for all $\dot{Q}$ with the exception of $\dot{Q}_{stored}$ used $T_{module,pre}$.

$$\dot{Q}_{stored} = \dot{Q}_{gain,sun} - \dot{Q}_{loss,\ elec} - \dot{Q}_{loss,\ natural}$$

From equation 5.1,

$$T_{module} = \frac{(\dot{Q}_{gain,sun} - \dot{Q}_{loss,\ elec} - \dot{Q}_{loss,\ natural})}{c_{panel} * m_{panel}} * t_{step} + T_{module,pre}$$

Estimating constants and coefficients:

The solar panel used in this model was the IM72 Series Photovoltaic Modules by MOTECH.

Solar panels were treated as black bodies with **emissivity and absorptivity**: $\mathcal{E} = \alpha = 1$

In literature [12], clear glass is usually given a **transmissivity** of: $\tau = 0.95$

Estimating the heat capacity of the solar panel:

$c_{panel} = \sum_m A d_m \rho_m C_m$ [13]

The two materials of the IM72 Module is polycrystalline Silicon and tempered glass [14]. Therefore, the equation for the specific solar panel will now be:

$$c_{panel} = A_{p-Si} d_{p-Si} \rho_{p-Si}\ C_{p-Si} + A_{temp,glass} d_{temp,glass} \rho_{temp,glass}\ C_{temp,glass}$$

$$A_{p-Si} = A_{temp,glass} = A = 1.95\text{m}^2$$

Tabulated values for parameters in c_{panel} calculation:

Material	ρ_m(kg/m^3)	C_m(J/ kg K)	d_m(m)	$Ad_m\rho_m C_m$(J/K)
Polycrystalline Silicon	2320	678	200×10^{-6}	613.54
Tempered Glass	2500	720	4×10^{-3}	14042

Table 5.1: Parameters for c_{panel}.

$$c_{panel} = \mathbf{14655\ J/K}$$

Due to difficulties in estimating **conductive and convective heat coefficients**, they were combined into one coefficient, h_{ck}. The solar panel surface area exposed to the ambient air is $2*A_{solar\ panel}$.

$$Q_{loss,\ natural} = (h_c + h_k) * 2 * A_{solar\ panel} * (T_{module} - T_{ambient}) + Q_r$$

$$Q_{loss,\ natural} = h_{ck} * 2 * A_{solar\ panel} * (T_{module} - T_{ambient}) + Q_r$$

The combined coefficient was estimated using data provided by Delaware Electric Cooperative on its solar farm, which utilizes the same model of solar panels.

If one side of the solar panel is exposed to wind, the other side will have only still air to convect heat away from its surface. Hence, the coefficients were expected to be higher than the free convection coefficient, somewhere close to the coefficients usually stated for low wind speeds due to the contribution of heat conduction [15].

Free convection = 5 W/m^2*C [15]

Forced convection at "low to medium wind speed"=10 W/m^2*C [15]

5 days were used to sample the h_{ck} values. The temperature data between 9am to 5pm were used to estimate the values of h_{ck} required to reach the recorded solar panel temperatures using the model.

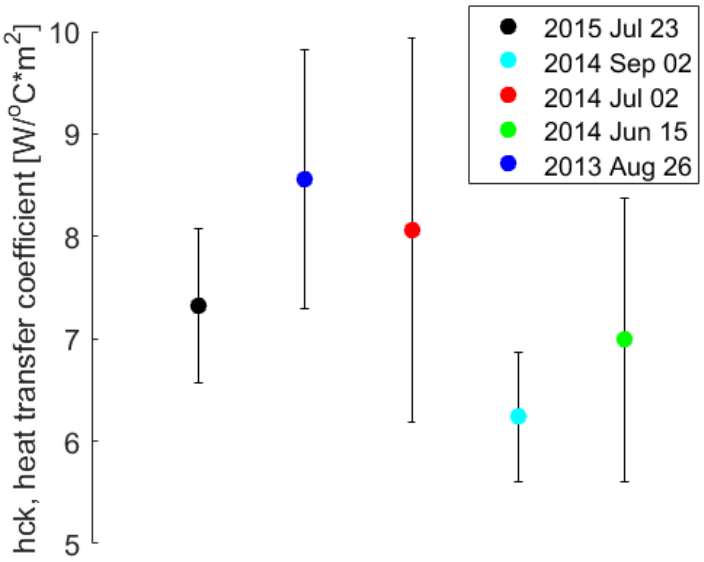

Figure 5.1: h_{ck} mean and standard deviation values (32 data samples each day).

The h_{ck} coefficients were within expectations and deemed stable enough to be used as a constant for the thermal model. The mean of the h_{ck} coefficients of 7.4352 W/m^2*C was used as the combined coefficient for the model.

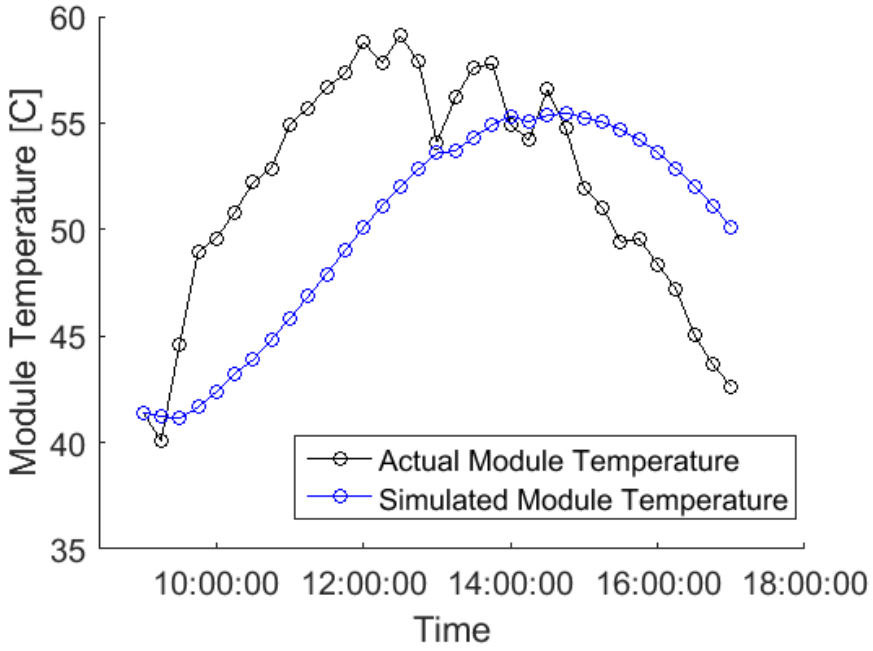

Figure 5.2: Comparing the actual module temperature to the simulated module temperature.

A possible reason causing the slight "lag" of the module temperature was the simulation assuming that all conditions were constant for the duration of a time-step (15 min). A solution was to shorten a time-step by extrapolating the conditions between each time-step.

Simulating operation of solar panel cooling in a Delaware solar farm using water evaporation

Assumptions:

1. Water evaporated completely within a time-step (15 minutes) from the solar panel surface.
2. Temperature changes of solar panel occurred in fixed time-steps (15 minutes). This meant that temperature remained constant until the next time-step begins.
3. Wind speed remained steady which corresponded to the combined heat transfer coefficient of 7.4352 $W/m^2°C$.

Using the above heat equations, the simulation was run for the day July 23, 2015 based on ambient temperature and irradiance data from the solar farm from 9am to 5pm. The cooling system attempted to keep the panel temperature below a threshold temperature differential with the ambient temperature. A range of threshold temperatures were simulated and the net profit resulting from the system was presented.

*dT = module temperature – ambient temperature

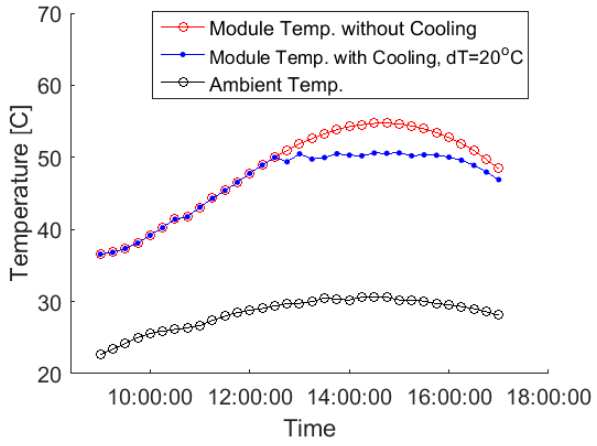

Figure 5.3: The module temperature with cooling (in red) to maintain a temperature differential of 20C with ambient temperature.

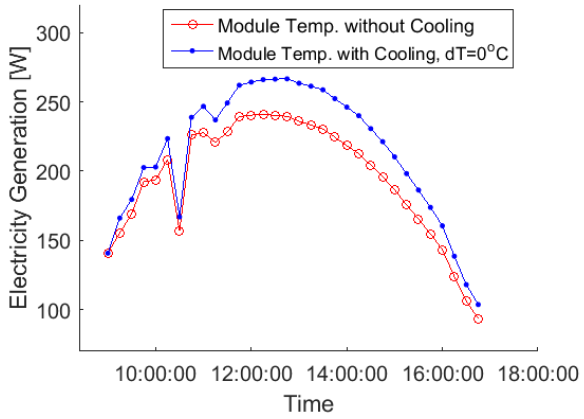

Figure 5.4: The power generated by cooling the module temperature to ambient temperature.

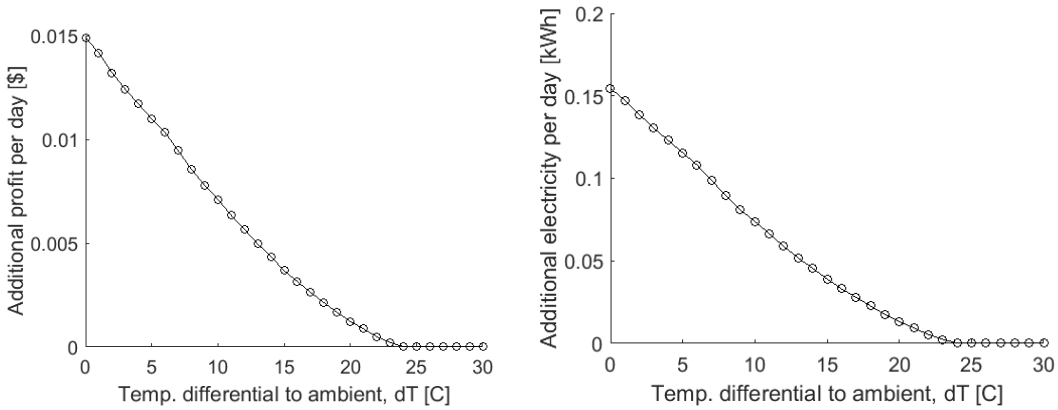

Figure 5.5: The additional profit and electricity to be maximum when module is cooled to ambient temperature

Simulation Results and Discussion

1. Max power gained: **0.155kWh/day**
2. Max profit gained: **$0.0149/day**
3. Cooled module temperature differential with ambient: **0 ºC**
4. Solar panel cooling using this method **increases power output** by up to **12%**.
5. The water required to keep the module at ambient temperature is **16.4 L** per day.

It is possible to cool the panel to an even lower temperature, up until what is known as the "wet bulb temperature". The missing component in this initial simulation was the rate of evaporation (which was assumed to be instantaneous), which would be the limiting factor of the minimum panel temperature. This was addressed during the water evaporation tests (next section) empirically, followed by a more robust theoretical approach to rate of water evaporation.

5.2 Initial Cooling Tests Using Different Methods

Water Evaporation

The first series of water evaporation tests involved the front panel surface heated up with a heat gun in an insulated chamber (Figure 5.6). There were 6 thermocouples distributed across the back surface of the panel to measure the panel temperature with respect to time. After reaching almost steady-state temperature, the back panel is sprayed droplets of water in fixed amounts and in fixed time steps.

Figure 5.6: Evaporative cooling test setup.

The rate of water evaporation was determined by measuring the time it took for the water droplets to evaporate at a given temperature (Figure 5.7).

The conductive heat transfer coefficient was assumed to be negligible due to the insulation of the chamber. The convective heat transfer coefficient was determined by treating the back of the solar panel as a flat plate in still air:

$L = \frac{A}{P}$, where A is the area of the back panel, P is the perimeter of the panel.

$T_f = \frac{T_\infty + T_{panel}}{2}$, where T_∞ is ambient temperature and T_{panel} is panel temperature.

Grashof number, $Gr = \frac{g\beta(T_{panel} - T_\infty)L^3}{v^2}$, where $\beta = \frac{1}{T_f}$, v is air's viscosity and g is gravitational acceleration.

Prandtl number, $Pr = \frac{c_p \mu}{k}$, where c_p is the specific heat capacity of the panel, determined by measuring the drop in temperature for every unit mass of water evaporated, k is the thermal conductivity of the panel material and μ is the dynamic viscosity of air.

Nusselt number, $\overline{Nu} = C(Gr\mathrm{Pr})^{m}$, can then be calculated, where C = 0.13 and m=1/3.

Finally, the convective heat transfer coefficient can be calculated, $\bar{h} = \frac{\overline{Nu}k}{L}$.

A heat transfer model was created based on the one developed for the solar farm's panels. The results were promising (Figure 5.8).

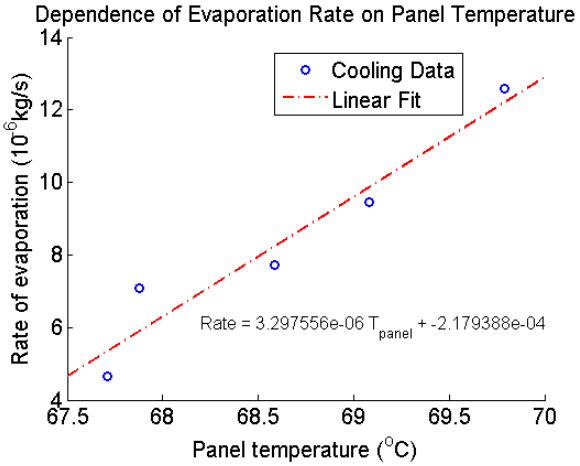

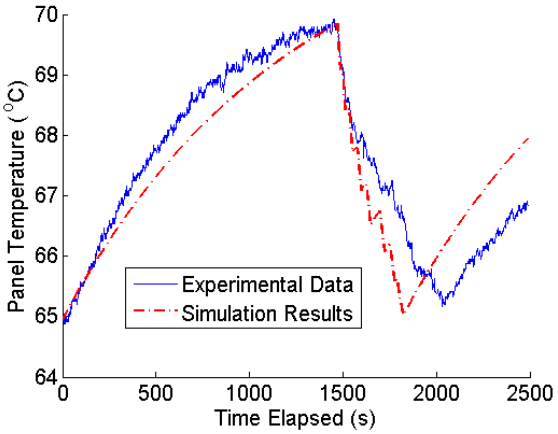

Figure 5.7: Empirical model of rate of evaporation ***Figure 5.8: Heat transfer model simulation.***

The empirical rate of water evaporation model seemed to allow the water to evaporate until the limit, wet bulb temperature. Hence, this limit and the amount of water required to reach the limit was used to determine the net savings from using evaporative cooling on a $2m^2$ solar panel.

Heat Fins

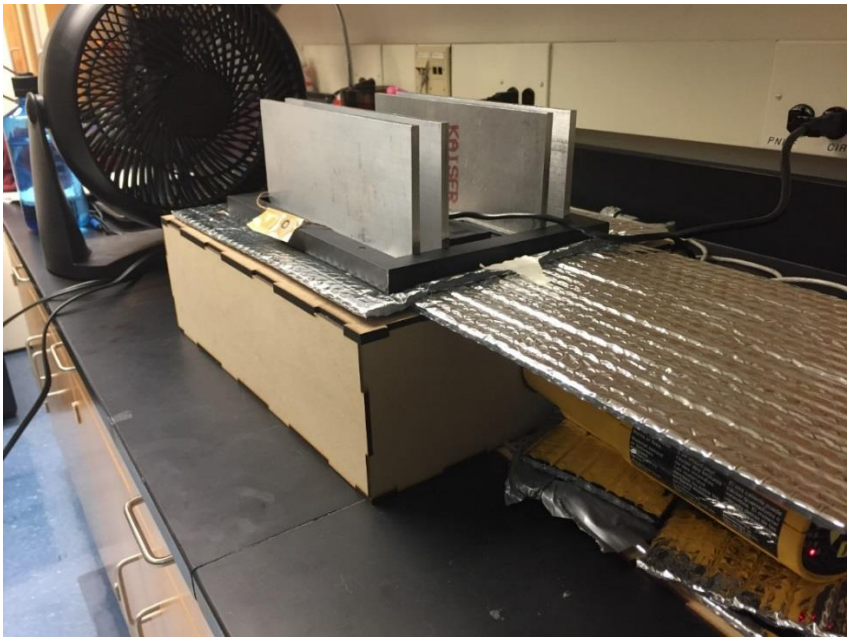

Figure 5.9: Test setup for the Heat Fins

The next method of cooling considered was the use of heat fins to passively cool the solar panels. Heat fins can be used to cool solar panels as the addition of the fins causes the back of the solar panel to have an extended surface. The extended surface increases the surface area that is exposed for cooling through convection and radiation. A set of four heat fins were manufactured out of aluminum to attach onto the small test solar panel. These fins were attached onto an aluminum plate that slid onto the back surface of the solar panel.

Tests were performed and a model was created to understand the heat transfer due to heat fins. The temperature difference due to the use of heat fins can be calculated by the equation shown below:

$$\Delta T = \frac{Q_{in} - Q_{out}}{m_{panel} c_{panel}}$$

Q_{in} is calculated from the hot air supplied from the heat gun once steady state temperature has been attained. Q_{out} is the heat transfer that occurs because of the increase in surface area when the fins are added in addition to convective and radiative heat losses. Equations related to the heat transfer due to the addition of the heat fins can be found in the Appendix. m_{panel} represents the mass of the solar panel and the additional heat fins while c_{panel} represents the specific heat capacity of the panel.

The test results and the simulation results showed that the heat fins had a temperature reduction of about 12°C.

Heat Exchanger

The last cooling method testing during the fall semester was creating an un-optimized heat exchanger to attach to the back of a smaller solar panel. A 3/8'' flexible copper pipe was used as the main mechanism for the heat exchanger because it is relatively inexpensive and has high thermal conductivity which made it ideal for the experiments. The heat exchanger was created by cutting and bending the copper pipe with the intent of maximizing the surface area in contact with the back surface area of the solar panel. The intent of the cooling method experiments was to achieve as close to maximum cooling potentials without optimizing for parameters such as cost or sizing of the system.

The solar panel was laid on top of an insulated box that only had one inlet and one outlet. The inlet allowed enough space for a heat gun to be inserted and heat the solar panel through the outlet that was as large as the front surface area of the solar panel that consisted of the glass surface and silicon cells. The heat gun was set at its lowest power setting in order to help the panel reach a steady state temperature. A plastic pipe was connected to a water faucet that applied enough pressure to run the water through the copper pipe. The copper pipe was laid on the back side of the panel which was filled with water in order to more evenly distribute the heat along the panel as opposed to relying on the contact between the copper and the back surface of the panel. Six thermocouples were used during the experiment to measure water temperature and panel temperature.

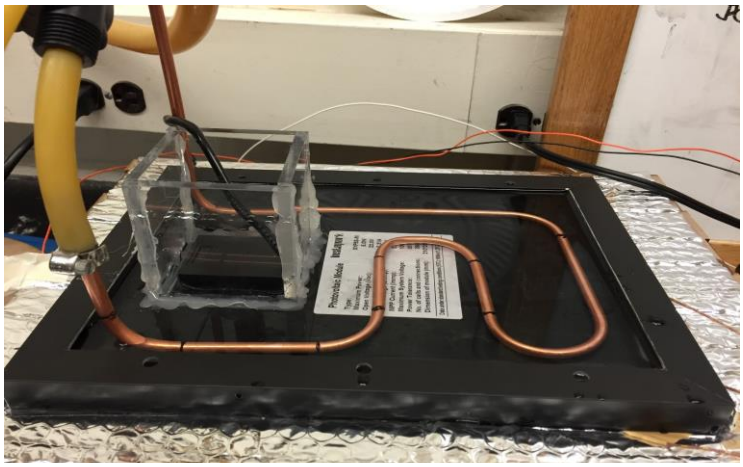

Figure 5.10: Heat exchanger test setup.

Three thermocouples were placed along the front side to measure the heated surface of the panel, two thermocouples were placed on the back surface of the panel to measure the cooled surface of the panel, and one thermocouple was used to measure the outlet water temperature which would be used to estimate heat removed with the heat exchanger. One of the front thermocouples would be sacrificed at the end of each experiment when the panel reaches a steady state temperature at the end of the cooling cycle in order to measure the mass flow rate of the water and to measure the inlet water temperature. It is found that both mass flow rate and inlet water temperature are directly related to the cooling of the panel. A maximum change in temperature of 20 °C was achieved and this difference in temperature is comparable to other heat exchanger tests performed in similar studies in other research papers. [16, 17, 18]

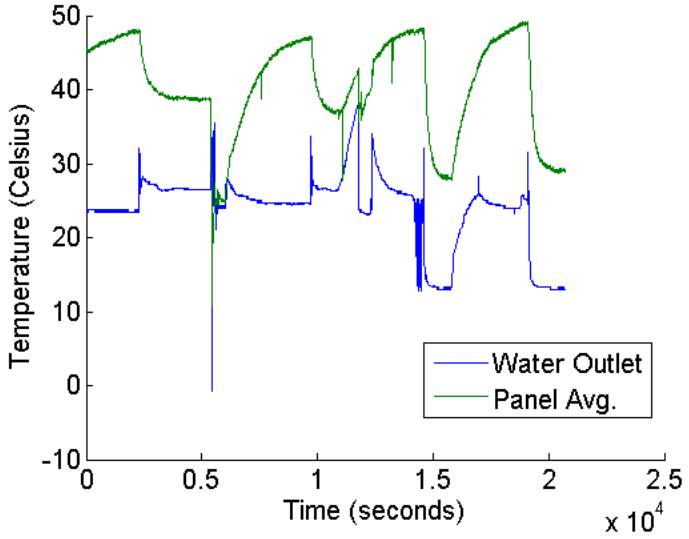

Figure 5.11: Test results for heat exchanger cooling.

Another finding from the experiment was that while the inlet water temperature was assumed to stay fairly constant, it actually increased in temperature over a long time period as it was running.

This increase in temperature heated the panel, which is important to take into consideration for scaling the system to a larger size. Ultimately it was decided that while the heat exchanger performed well in cooling the solar panel, it would require a significant amount of resources to implement compared to the other cooling methods: heat fins and evaporative cooling. There would have to be significant modifications to the panel to contain the heat exchanger in an insulated area on the back of the panel and it will require a significant amount of water for the system to work effectively. It may have been possible to further optimize the experiment and the final large scale version of the heat exchanger; however, due to time and budget constraints, it was decided that the evaporative cooling method would be the most promising to continue further and optimize.

Cost Analysis of the Three Cooling Methods

Overall, a cost analysis was performed on the impact of the three different cooling methods. The cost model was performed for one solar panel over its lifetime with an efficiency of 20%. Each cooling method described above results in the solar panel to be cooled to a maximum difference in temperature (delta T). This cooling will result in an increase in the power output of the solar panel, which will result in an increase in savings. However, each cooling method also has specific costs related to the manufacturing, installation, and use of the system. With the evaporative cooling method the cost of use will be related to the amount of water that will be used, with the heat fins the main cost is related to the use of the aluminum fins, and with the heat exchanger the main costs are with the use of water and the copper piping. Thus, these costs are taken into account in addition to the savings generated from cooling the solar panel to find the profits that can be generated by these three cooling methods. The results of the findings are shown below.

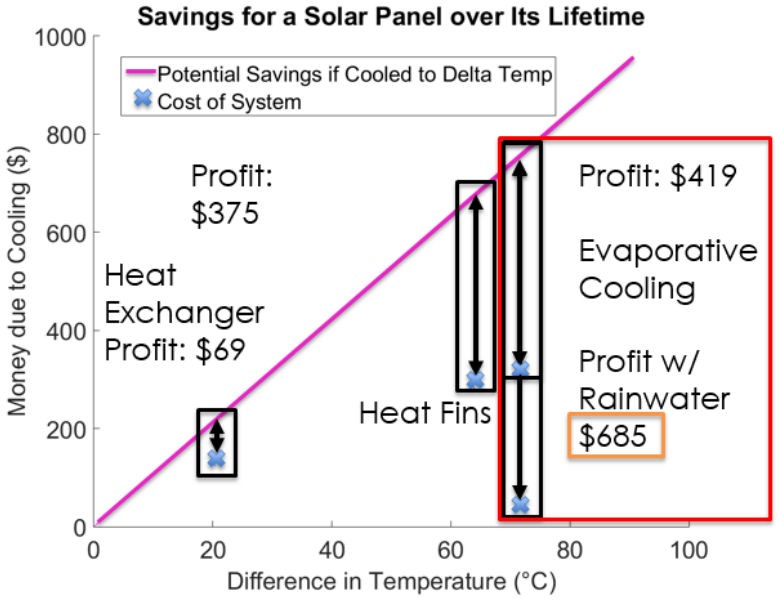

Figure 5.12: Cost Analysis of Different Cooling Methods

The results of this cost analysis show that evaporative cooling would be the most profitable means of cooling. Thus, the proposed solution of cooling would utilize a form of evaporative cooling.

5.3 Wicking

Even though the results of the different cooling methods showed that spray cooling through evaporation would be the most cost effective, this form of cooling resulted in mineral deposition on the surface of the solar panel. As the water evaporated, the mineral residue in the water remained on the surface of the panel. This will eventually lead to the clouding up of the surface of the PV cells, which will impact the power generation of the modules. In addition, the construction of this spray system would prove to be difficult to manufacture for a large solar farm setting. Therefore, an alternative form of evaporative cooling was examined known as wicking. This process of evaporative cooling uses capillary action to transport water through cotton that is placed on the backside of the solar panel. As the water travels through the cotton, the heat of the solar panel will evaporate the water. Important characteristics of wicking needed to be understood before creating a design for the system.

Characterization of Wicking Rate

The project investigated two different, but closely related wicking rates:

1. Wicking Displacement Rate: The velocity that water travels through a wicking fabric.
2. Wicking Volume Rate: The total amount (volume/mass) of water that travels through a wicking fabric in a given time.

Wicking displacement rate was used as a relatively fast characterization parameter to determine the desired wick material. Then, after the ideal wick material has been chosen, lengthier tests were performed to determine its wicking volume rate, which is required for the final system design.

Wicking Direction

- Upwards
  Tests were performed to study the properties of upwards' wicking rate using a simple test setup as shown in Figure 5.13. The wick fabric was dipped in dyed water while being held up vertically. The fabric was marked at intervals of 3cm. The time was recorded when the water reaches a marking. The displacement between markings was divided by the time it took for the water to reach each marking to get the displacement rate.

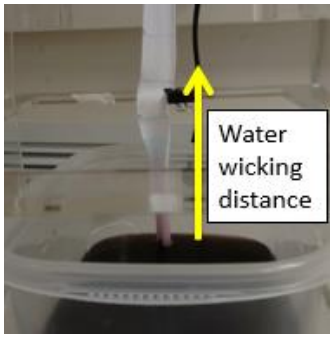

Figure 5.13: Upwards wicking test setup.

- Downwards
  The test setup to study downwards wicking was similar to the upwards test setup, but instead of being held vertically upwards, the wick fabric was let down over the rim of the water container. This introduced an additional parameter—the water uptake height, as seen in Figure 5.14. The water uptake height is the vertical distance that water travel upwards through capillary action before wicking downwards through the rest of the wick fabric's length. The relationship between the water uptake height and the wicking displacement rate was investigated as well.

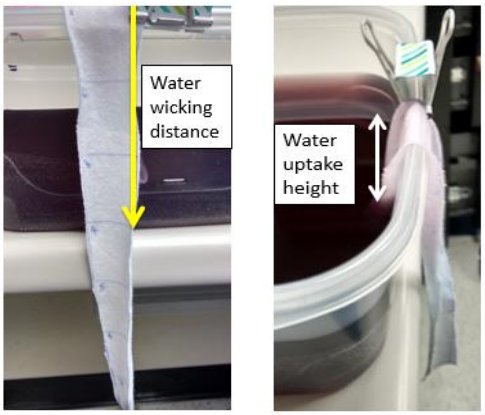

Figure 5.14: Uptake wicking test parameters.

Results and Discussion

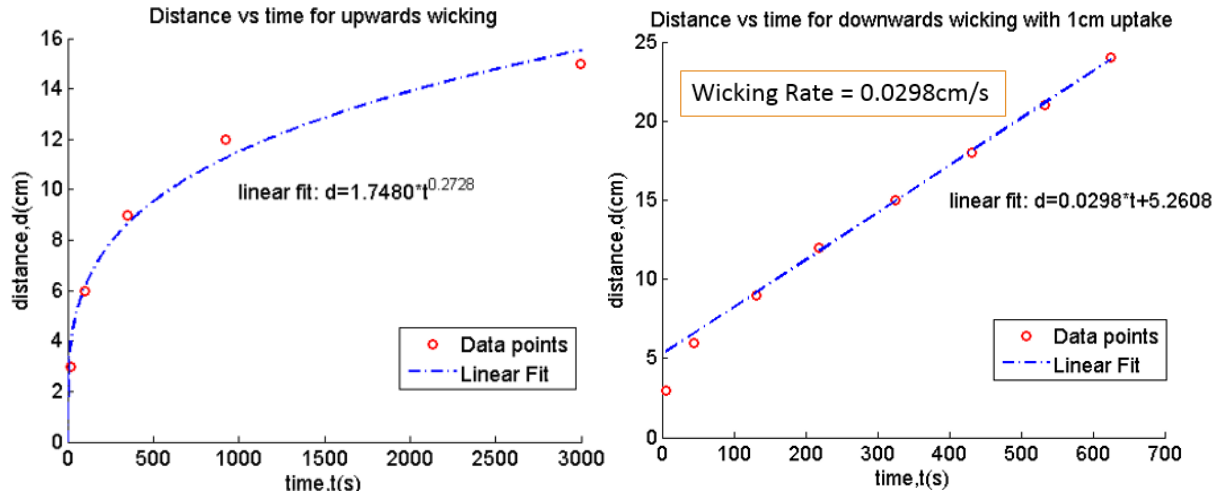

Figure 5.15: Upwards and downwards wicking results.

From the plot in Figure 5.15, upwards wicking has the property of slowing down as the distance travelled increases. In contrast, the downwards wicking rate remained constant after a short transient period during which the wicking rate decreases. The constant rate of downwards wicking allows for easier wicking rate predictions and scaling the wick fabric's length. Due to the rate of upwards wicking decreasing with distance, water was only able to travel only 50cm in an hour. On the other hand, downwards wicking rate remained constant after a short initial transient period, making it ideal for the EvaporaSun system as the average solar panel is 2-by-1 meters in size and the system requires the water to travel through the entire length of the solar panel.

Hence, downwards wicking was selected as it has a constant rate of wicking regardless of distance along with it being able to wick further and faster.

Wicking Material

2 different fabric **material compositions** were tested for their wicking displacement rates.

Fabric	**100% Cotton**	**35% Cotton, 65% Polyester**
Wicking Rate (cm/s)	$5.6*10^{-2}$	$<2.8*10^{-3}$

Table 5.1: Wicking rate of different material compositions.

As the cotton-polyester mix's wicking rate was at least an order of magnitude slower than the 100% cotton fabric, cotton was chosen as the wick material.

Two different **knit structures** were then investigated for cotton fabric.

Fabric	**Ribbed Cotton**	**Plain Cotton**
Wicking Rate (cm/s)	$1.4*10^{-1}$	$4.3*10^{-2}$

Table 5.2: Wicking rate of different knit structures of cotton.

As ribbed cotton wicks faster than plain cotton, ribbed cotton was chosen as the wick fabric to be used in the system.

Modelling of Downwards Wicking Rates vs Uptake Height

Tests were performed to attain a model for downwards wicking rates vs uptake height.

Material: Ribbed Cotton

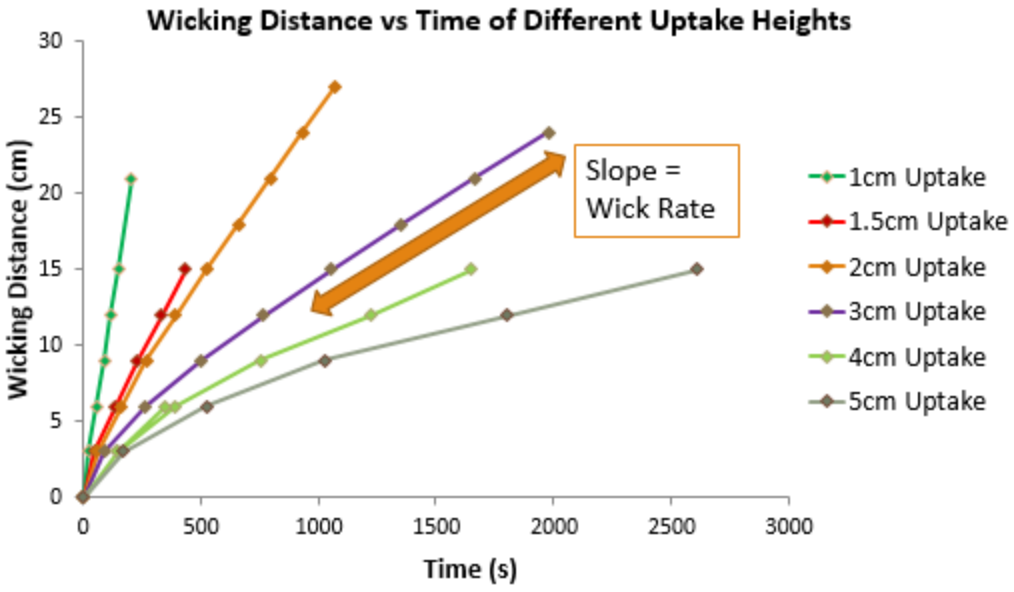

Figure 5.16: Wicking distance vs time at different uptake heights.

By extracting the steady-state wick rate from each of the uptake heights, a power law relationship was found between wicking rate and uptake height (Figure 5.17).

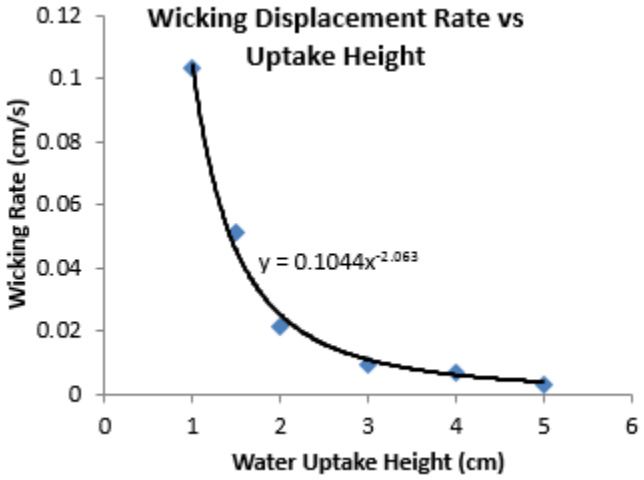

Figure 5.17: Wicking rates vs uptake height.

The wicking volume rate was determined for a ribbed cotton sheet placed at 30^{o} angle from horizontal. An empty container was first measured on a mass balance before allowing the water wicked through the length of the wick material to drip into it. After a span of time (usually 15 minutes), the container is weighed again. The difference in mass is divided by the time elapsed to get the wicking volume rate for that particular uptake height. As expected, the wicking volume rate vs uptake height also exhibit a similar relationship:

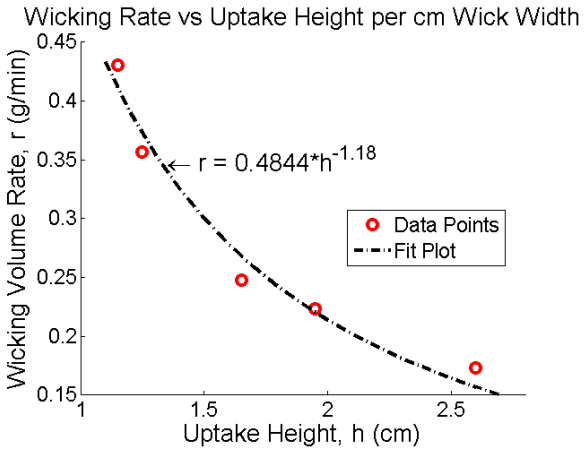

Figure 5.18: Wicking volume rate vs uptake height.

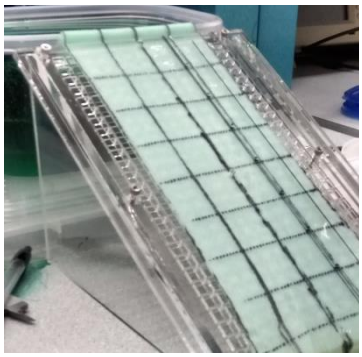

Figure 5.19: Wicking volume rate test setup

The **effect of strain** along the fabric's width on its wicking rate was also investigated (Figure 5.20). The strain on the cotton was maintained using clips (Figure 5.21).

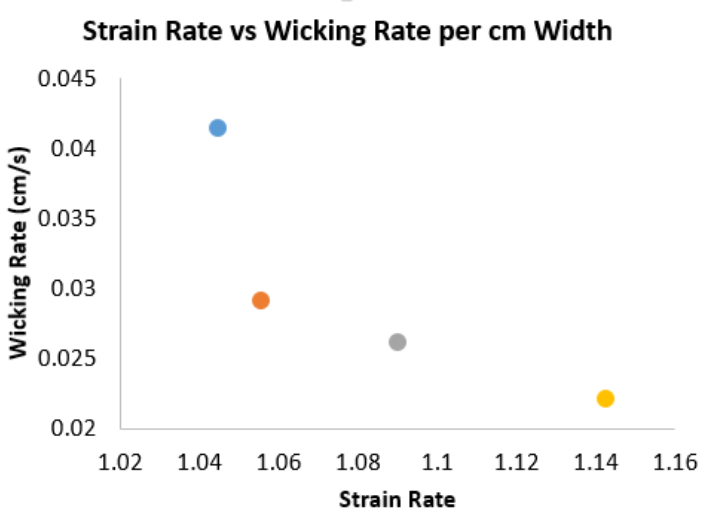

Figure 5.20: Wicking rate vs strain rate results.

Figure 5.21: Wicking rate vs strain rate test setup.

This demonstrated that care must be taken to maintain a constant stress/strain on the fabric when using it to wick water in the system. As such, to simplify matters, the wick fabric was not placed under any stress along its surface.

5.4 Water Transmission

Once the process of wicking was fully characterized, the next step was to make design decisions related to whether to use power to control the water supply, which is a form of active cooling, or using mechanical systems or natural elements to control the water supply, which is a form of passive cooling. Therefore, different kinds of control mechanisms for the transmission of water to the cotton wick were considered and show below:

Type	Active/Passive	Pump Needed?	Estimated Cost	Robustness
Pressure Sensor	Active	Yes	$35	Sensor can be affected by overflow of water.
Load Cell	Active	Yes	$10	No moving parts; Large Capacity.

Ultrasonic Sensor	Active	Yes	$2	Protect it from water touching it.
Ball Valve	Passive	No	$10	Lasts for a long time (used in toilets)
Float Switch	Active	Yes/No	$10	As long as the electronics don't get damaged.
Check Valve	Passive	No	$7	Long lifetime.

Table 5.3: Design Table for Water Transmission

More information regarding the function of these various control mechanisms can be found in the *Appendix*. Based on the robustness of the system, the passive control mechanisms trumped the active control mechanisms. The check valve cannot be used by itself; therefore, the decision to go with the float valve to control the water was made. The water is stored in a unit known as the wick containment unit (WCU). Therefore, this float valve regulated the water level in this WCU.

5.5 Water Storage

After it was finalized that the EVA system would ultimately use water to cool the solar panel, plans for reducing water consumption were made. A study was performed to test the feasibility and cost difference that an addition of a rainwater collector can have on the EVA system. For the study, areas in the US were chosen based on optimal values of both annual precipitation and annual insolation which were found in Florida, Louisiana, and Texas. More information regarding this data can be found in the *Appendix*. To reduce the cost of the rain water collector, a 55-gallon water barrel was used as the collection tank because it is a common item that can be found for prices as low as $10 per barrel. The majority of the cost of the rain water collector, however, will come from the support structure for the water barrel which was estimated to be $50 using a simple wood structure. The savings from utilizing the rain water collector will determine whether or not it is worth further optimizing the design.

The study was conducted by first setting an assumption of 65 inches of rainfall per year and that one rain barrel will be utilized for each rain water collector.

5.6 Small Scale Prototype

The small prototype the WCU was designed so that experiments could be performed with the small solar panel to determine parameters such as wicking rate and rate of evaporation. In addition, the prototype would be used to validate the model under both an indoor controlled testing setting and outdoor testing conditions. The main design criteria that went into creating the small prototype of the WCU were the following:

1. Fit within the testing rig
2. Attach onto the solar panel without any modifications to the solar panel itself.
3. Orient upright when the solar panel is at a 30 degree slant, which is the typical orientation for solar panels to receive the most incoming solar irradiation throughout the day.
4. Opening for the wick to come out onto the back surface of the solar panel without being exposed to the outside environment.
5. Hole for the float valve to fit onto the inside of the unit.
6. Fit compactly behind the solar panel so as to not create any shadows on the surface of the panel or obstruct the solar panel from absorbing the incoming solar irradiation.
7. Easy to manufacture.

The above listed design criteria led to the following design for the small scale prototype of the WCU:

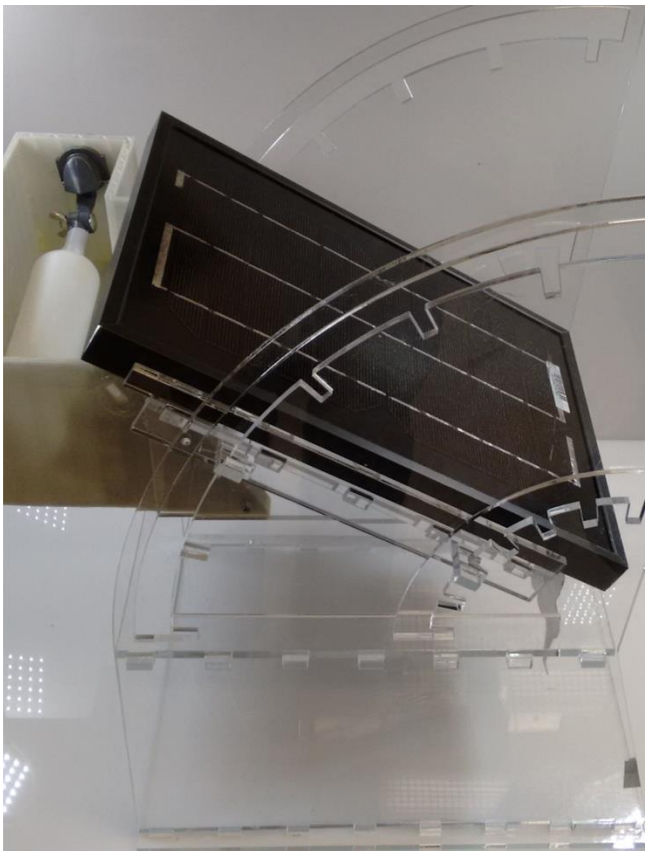

Figure 5.22: WCU attached onto the test rig with the solar panel

Figures 5.23: WCU side view (left) and WCU top view (right).

The WCU was 3D printed with PLA using the Taz Bot. The choice to go with 3D printing over laser cutting was due to the need of waterproofing the WCU so that no water will leak through. Once it was 3D printed, the interior of the WCU was water proofed. Due to the ease of manufacturability, a rectangular design was chosen for the storage of the water behind the solar panel. This rectangular storage vessel allowed for the WCU to easily slide behind the solar panel without obstructing its ability to generate power. The wedges that sprout out of the rectangular storage vessel have an incline of 30 degrees so as to easily slot onto the back of the solar panel where it was attached to the test rig with screws. Tapped 4-40 plugs were inserted into the WCU so that it could screw onto the test rig. Finally, there was no lid for the WCU to enclose it so that changes in the water level could be observed as the wicking process occurs during testing.

5.7 Medium Scale Prototype

After completing a prototype and running experiments on the system, it was thought to be suitable to scale up incrementally to a medium scale system. The hope would be to establish a verification of the system working at larger scales. A 100 W solar panel was purchased to build the EVA system due to budget and time constraints nearing the end of the spring semester. A full scale system would utilize a 250 W panel which would better represent the size of the panel for a solar farm. The end goal for the project will be to implement the EVA system for a large scale solar farm in order to realize significant cost savings that would otherwise not be realized in a residential application.

The general process of the system is illustrated in Figure 5.24. It will take an input of municipal water that is then distributed through cotton wicks that are attached to the back of a solar panel. Once the water reaches the back of the panel through the cotton wicks, the heat from panel evaporates the water in the cotton wick and in effect cools the panel to a lower temperature. Several considerations were taken into the design of the system. The primary factor that influenced the design was reducing the cost of the overall system. Because of this, low cost materials were used and the system was made to be as passive as it could to cool the panel.

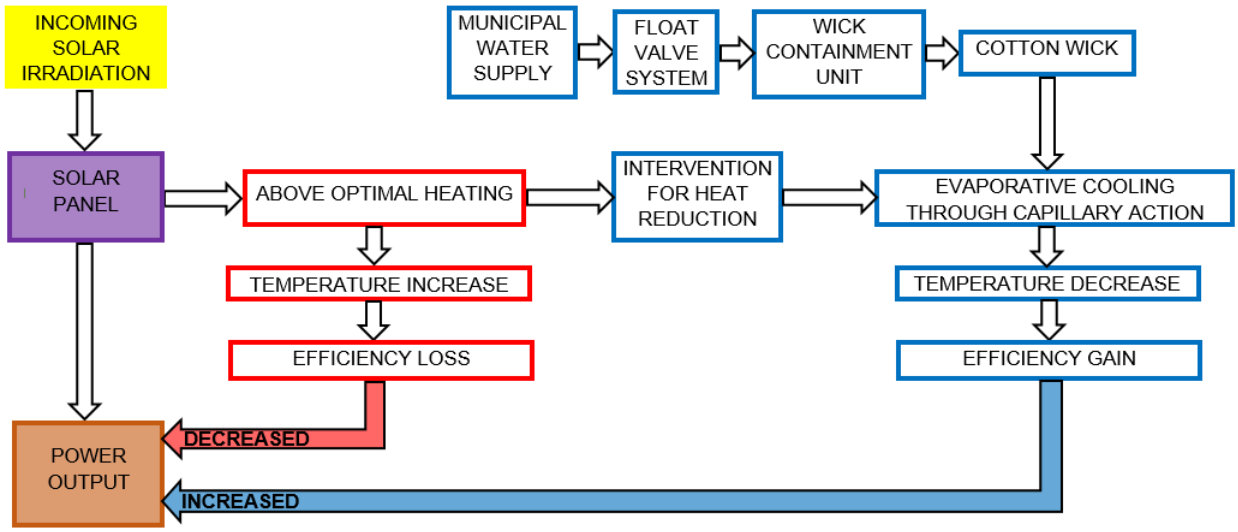

Figure 5.24: System flow chart.

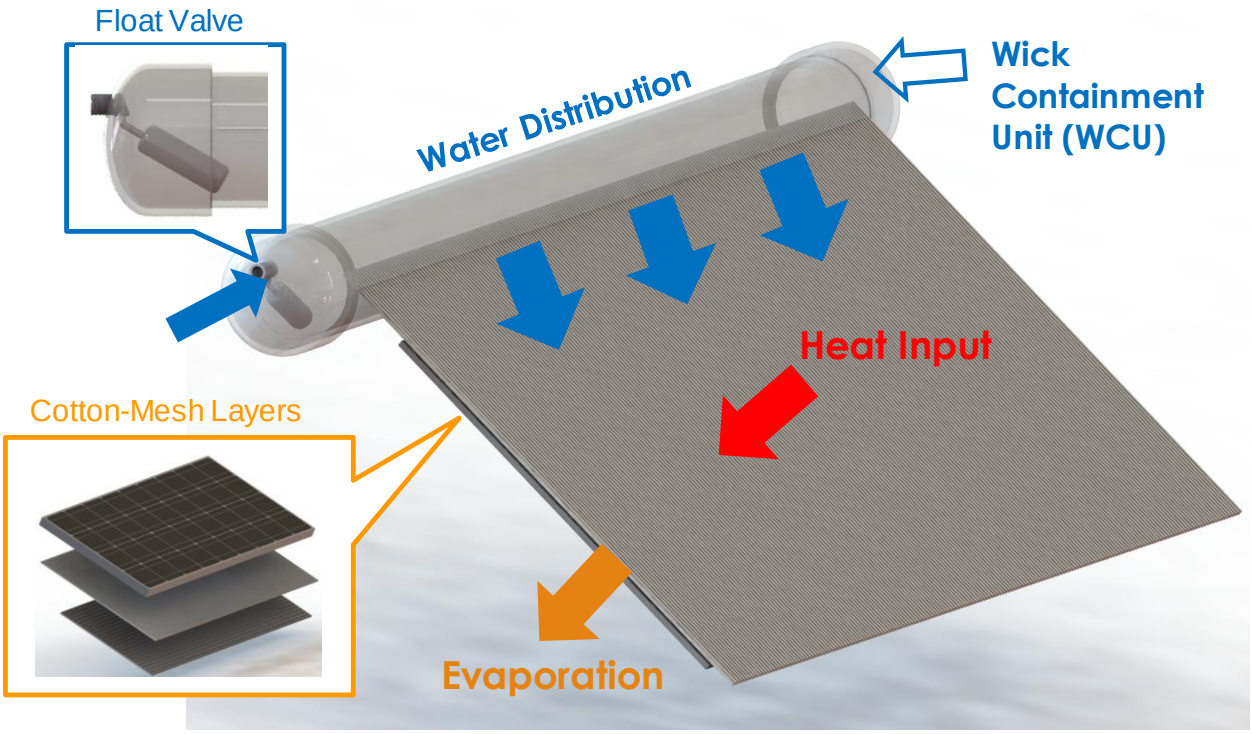

Figure 5.25: System breakdown.

The first component considered was the method of controlling the amount of water for the system. Designs that were considered to control the amount of water delivered to the back of the panel for evaporative cooling included electrically actuated valves and float valves. It was decided to implement the use of the float valve because it requires no energy input to control the water level within the WCU. A simple float valve was utilized because the pressure from the municipal water supply, typically between 30 to 80 psi, was not large enough to warrant the need for larger or more expensive float valves.

The size and the movement of the float valve then dictated the size of the WCU that contains the water and the inlet of the cotton wicks for the EVA system. A size 4 PVC sewer pipe was used to construct the WCU because of its light weight, low cost, and ability to fit the movement of the float valve attached at the end cap. The length of the pipe was cut to match the length of the solar panel and had a thin slit cut along its length to fit the inlet of the cotton wick. There is also a matching thin slit cut along the edge of the solar panel to minimize the amount of cotton exposed to the environment and to minimize the uptake height that is experienced outside of the WCU. The uptake height is important for controlling the amount of water transported from the WCU to the solar panel; however, it should only be established inside the WCU in a controlled environment as opposed to outside of the WCU. Having an uptake height for the water to travel through the cotton outside of the WCU runs the risk of the water evaporating in the environment before the water reaches the backside of the panel.

The cotton is then laid across the back of the panel to distribute the water evenly. It is seen from previous experiments that the wicking rate of the cotton is affected by the amount of force applied to stretch it. This insight suggests that the cotton cannot be stretched out and bolted to the back of the panel as originally planned. The reasoning for this effect may be caused from the ribbed cotton having small channels that are flattened when stretched. This will then cause the capillary effect that allows the water to travel through the cotton to be reduced and make it more difficult for the water to transport along the cotton ribs.

In addition, another issue that needed to be addressed was regarding the cotton attaching onto the solar panel's back surface. It is important that the cotton is always in contact with the back surface to be most effective. This issue was resolved by adding a thin mesh that would press the cotton sheet onto the surface of the back panel and also allow for convective heat transfer to let the water evaporate to the environment.

Four different mesh materials were compared with each other to be used for the back of the solar panel. They were compared based on the available pore size, flexibility, temperature it was able to withstand, and cost. A polypropylene perforated sheet was chosen because it performed better in most of the categories compared to the other materials considered. While its bending was minimized, when scaled to the medium scale panel, it slightly bowed in the middle of the back of the panel. This was resolved by applying thin acrylic strips along the centre of the panel where bowing was most prevalent.

A rack was then designed from acrylic to hold the WCU along the back side of the solar panel. The WCU and the rack were circular fits so that the angle of descent for the cotton from the WCU can be adjusted no matter what angle the solar panel was fixed at. The WCU simply rotates on the rack that is screwed to the panel and, hence, it is always parallel to the back surface. While this rack design works for the particular solar panel framing for the medium scale system, it was difficult to design a universal rack system for solar farms because different solar farms use different framing systems.

The medium scale EVA system would be use to validate the assumption that results from the small scale tests could be scaled to larger systems such as 250 W solar panels used in solar farms.

SECTION 6:
VALIDATION

6.1 Heating-Cooling Tests with Small Scale Prototype

After completing the characterization of wicking rate, heating and cooling tests were conducted to investigate the behavior of the effect of water evaporating from the wick fabric has on the temperature of a solar panel.

Test Setup

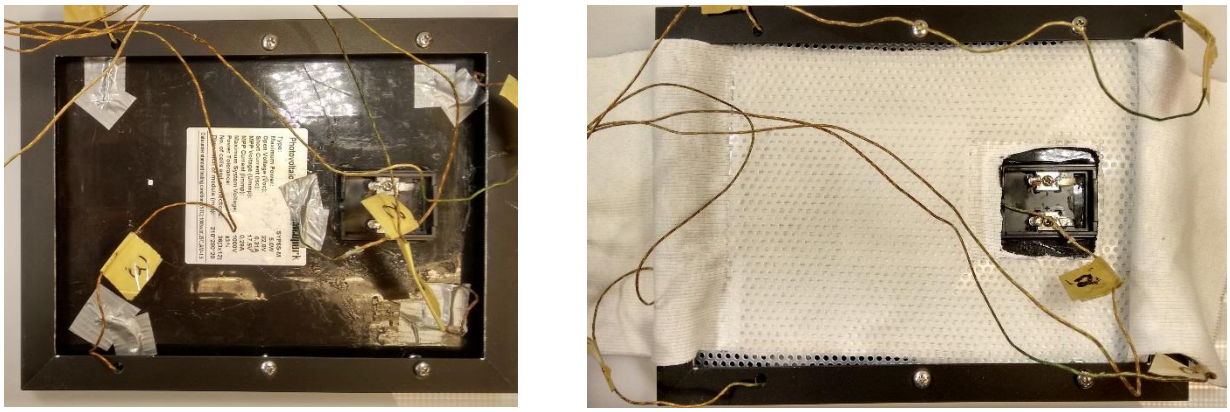

Figure 6.1: Back of solar panel with thermocouples, cotton wick and mesh support.

Measurements/Readings

The **temperature readings** were taken using 5 thermocouples at the back of the solar panel (Figure 6.1), with one thermocouple used to record the ambient temperature. The thermocouple breakouts were connected to an Arduino Uno (Figure 6.2), where the temperature readings were then recorded with timestamps on a computer with a program, Gobetwino, interfaced with the Arduino serial output. Plots of the temperature readings on all 5 thermocouples can be viewed real-time using a custom MATLAB script.

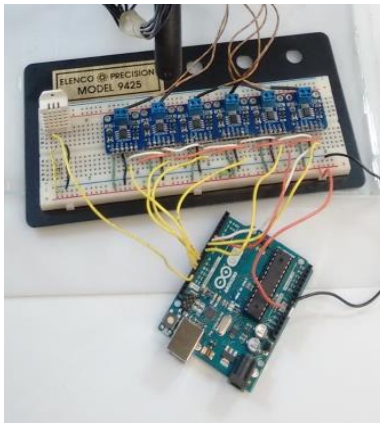

Figure 6.2: Electronic sensors to measure humidity and temperature.

Relative humidity readings were taken using a DHT 22 temperature and capacitive humidity sensor similarly interfaced with the computer through an Arduino Uno.

Mass readings of water with its container were measure using a digital mass balance with resolution of up to 1g.

Wick Fabric Fixture

The wick fabric was placed over the thermocouples and fixed onto the back of the solar panel with a porous acrylic sheet pressed gently against the wick fabric using nuts and bolts. This is to ensure that the wick fabric is in constant contact with the back of the solar panel while allowing evaporation to occur through the pores of the acrylic sheet. This also prevents stress and strain

along the surface of the wick fabric as it had been shown to decrease its wicking rate (refer to Modelling Wicking Rate vs Uptake Height).

Heating

Figure 6.3 is the heating test setup, with the heat sheets (in orange) providing heat to the solar panel. An intermediary aluminum plate was used to distribute heat more evenly across the solar panel's surface. Only 3 heat sheets were connected to the power supply for each test, supplying the amount of heat that the solar panel is estimated to receive under direct radiation of 900W/m^2 (See calculation below).

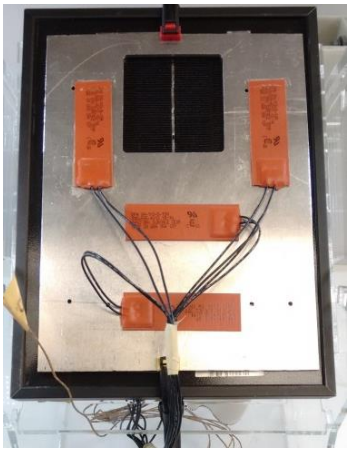

Figure 6.3: Heating setup.

Solar panel area [m^2]	0.058548
Peak solar irradiation [W/m^2]	900
Solar Panel Efficiency	0.2
Solar Radiation converted to heat [W]	**42.15475**
Heat Supplied (1 Heat Sheet) [W]	15
Heat Supplied (3 Heat Sheets) [W]	**45**

Table 6.1: Calculation for number of heat sheets required to simulate solar irradiation.

Cooling

After the panel is heated for approximately an hour when the panel temperature had almost reached steady state, the top end of the wick fabric is then dipped into the water with a fixed uptake height. Excess water is collected at the bottom of the wick fabric using a pre-weighted container. As the test progressed, the water stored in the Water Containment Unit (WCU) was constantly refilled from a bottle to maintain a fixed uptake height.

After the cooled panel's temperature reached steady state, the timer starts. At the start of each test, the bottle and the empty excess water container were weighed using the mass balance. After 15-20 minutes, the timer is stopped and the bottle and the now-filled water container were weighed again. The difference in the bottle's final and starting weight is the total amount of water wicked through the fabric at the given uptake height. Dividing that by the time elapsed gave **the wicking rate of the wicking fabric**.

On the other hand, the collected excess water's weight was subtracted from the bottle's reduction in weight to get the total amount of water evaporated from the back of the solar panel. Dividing the evaporated water by time elapsed gave the **water evaporation rate**. To account for the evaporation of water from the containers, a **control** consisting of an identical water container filled with water was set up during each test. It was determined that the evaporation from the container was negligible as each time it was less than 4% of the total water evaporation.

Results/Discussion

Water evaporation rate remained 24-26 g/min under similar conditions (slight differences in ambient temperature and relative humidity) using the ribbed cotton as well as a spandex-cotton fabric mix at different wicking rates but still saturated (excess water was still collected in the container). This result agreed with the assumption made that the water evaporation rate remains the same regardless of wicking rates as long as the fabric is saturated. This means that the maximum water evaporation was reached in each of the cases.

The heating-cooling tests produced **temperature plots** such as in Figure 6.4. On average, the temperature of the panel decreased by 15ºC with Eva from the maximum temperature without Eva.

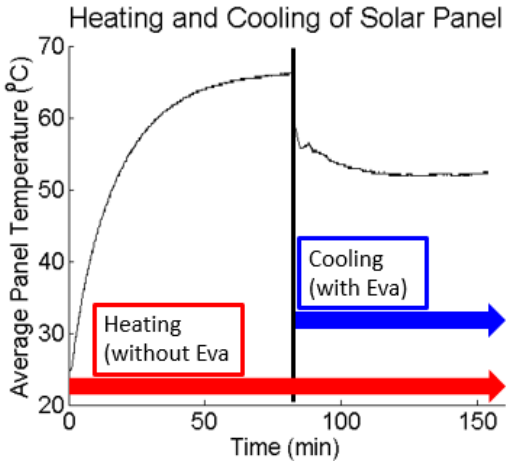

Figure 6.4: Heating-cooling test average temperature plots.

A **heat transfer model** was created for the solar panel using the Eva system based on the one developed during an earlier part of the project (refer to "Preliminary Tests: Evaporative Cooling"). The difference was in the rate of evaporation. **A theoretical model for rate of evaporation** was used instead of the empirical model used in the earlier version as the theoretical model accounts for atmospheric pressure and relative humidity, both of which was not included in the empirical model due to resource and time constraints. The theoretical model was based on the Penman Equation modified by W. Jim Shuttleworth in 1993. Figure 6.5 shows the results of a MATLAB simulation using the heat transfer model, which agreed well with the experimental results.

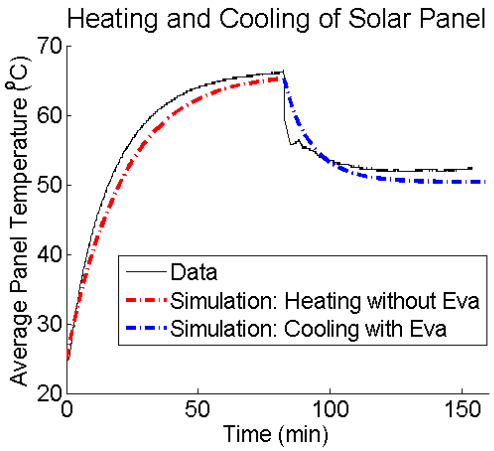

Figure 6.5: Simulation results overlapped with test results.

6.2 Steady State Cost Optimization Model

A cost optimization model that maximizes the cost benefit of the EVA system in a solar farm setting was created based on the wicking rate and rate of evaporation that were experimentally determined. The main constants that need to be defined are the ambient temperature and the surface area of the solar cells of the solar panel. The surface area of the solar cells is determined by the surface area of the whole solar panel multiplied by the manufacturer defined fill factor for that particular solar panel. The optimization model goes through a range of wick uptake heights and wick uptake percent coverages, which is the amount of cotton that is dipped into the water in the wick container unit compared to the surface area of the solar panel.

For these range of uptake heights and wick uptake percent coverages, the amount of water consumed is calculated. An assumption this model makes is that the amount of water consumed is equal to the wicking rate, which is a function of the uptake height. Therefore, this rate of water consumption is evaluated in terms of kg/s. In addition, this rate of water consumption is dependent on how much the wick uptake percent coverage is. This value of wick uptake percent coverage is multiplied to the rate of water consumption to find the actual amount of water the system will consume. When the wicking rate was evaluated, the tests consisted of the all the cotton wick submerged in the water. Therefore, if the wick uptake percent coverage is reduced by a certain percentage, the amount of water consumed by the system will also be reduced by the same percentage For example, a 70% wick uptake percent coverage will cause the amount of water consumed by the system to reduce by 30%. This water consumption rate is compared to the maximum rate of evaporation of water. When the maximum rate of evaporation of water is greater than the rate of water consumption, then the current rate of evaporation is equivalent to the rate of water consumption. On the contrary, if the maximum rate of evaporation of water is smaller than the rate of water consumption, the maximum rate of evaporation of water is used as the current rate of evaporation. Just like for the small scale testing, the maximum water evaporation rate was calculated using the theoretical model based on the Penman Equation modified by W. Jim Shuttleworth in 1993.

For this particular optimization model, a major assumption that was made was that the system is operating at steady state conditions as the rate of evaporation was evaluated at steady state conditions. In addition, the largest difference in temperature is evaluated when the cotton wick is

completely saturated. Therefore, to find the temperature of the solar panel, the steady state heat equation is used. When the Eva system is in place, the heat equation is evaluated to be **Equation 6.1**. The heat loss due to radiation is given by **Equation 6.2** where ε is the emissivity of the solar panel is, σ is the Stefan Boltzmann constant, and A is the surface area of the solar cells on the solar panel. The heat loss due to convection is given by **Equation 6.3** where h is the convection coefficient based on the outside ambient conditions. Finally, with the Eva system, there will be additional heat loss due to evaporation. This heat loss due to evaporation is given by **Equation 6.4** where h_{latent} is the latent heat of water, which means the amount of energy that is released as water changes from liquid to vapor, and $\dot{m}_{evaporation}$ is the rate of evaporation. The only unknown in these set of equations described above is the temperature of the solar panel; hence, the steady state heat equation is used to evaluate this variable. When the Eva system is not in use, the same heat equation can be used to evaluate the temperature of the solar panel for the various ranges of uptake height and wick uptake percent coverage using **Equation 6.5**.

$$Q_{in} = Q_{out} = Q_{rad} + Q_{convecion} + Q_{evaporation} \qquad Equation\ 6.1$$

$$Q_{rad} = \varepsilon\sigma A\left((T_{solarpanel}\right)^4 - ((T_{ambient})^4) \qquad Equation\ 6.2$$

$$Q_{convection} = hA\left(T_{solarpanel} - T_{ambient}\right) \qquad Equation\ 6.3$$

$$Q_{evaporation} = h_{latent}\left(\dot{m}_{evaporation}\right) \qquad Equation\ 6.4$$

$$Q_{in} = Q_{out} = Q_{rad} + Q_{convecion} \qquad Equation\ 6.5$$

Once these temperatures are found (temperature of the solar panel with Eva and temperature of the solar panel without Eva), the cost analysis portion of the optimization model can be evaluated. First, to evaluate the amount of money spent on water, the amount of water consumed is multiplied by the cost of water over the course of the operation of the Eva system. In this analysis, one of the assumptions made is that the Eva system will operate only during the time when the Sun is out. Therefore, coordination with the solar farm staff is necessary to make sure that the municipal water supply is on during the daytime and off during the night time.

The next step is to evaluate how much money is generated by the production of electricity by these solar panels. The amount of power generated by the solar panel without the cooling system integrated is as shown in **Equation 6.6** where I is the incoming solar irradiation. As stated earlier, the solar panel's rated efficiency drops by 0.45% per degree over the reference temperature of 25℃. Therefore, based on the temperature of the solar panel, the amount of power generated by it will change. This loss in efficiency needs to factor into calculating the present efficiency of the solar panel under the given temperature and solar irradiation. Hence, the new reduced efficiency is given by **Equation 6.7** and this new reduced efficiency is inputted into the equation evaluating the power generated by the solar panel.

$$P_{solarpanel} = \eta_{reduced} I\varepsilon A \qquad Equation\ 6.6$$

$$\eta_{reduced} = \eta * \left(-0.0045 * \left(T_{solarpanel} - 25℃\right)\right) + \eta \qquad Equation\ 6.7$$

Based on the price of electricity and the number of hours of sunlight, the amount of money generated by this power production can be evaluated. The amount of money produced due to the

power generated by the solar panel with the Eva system is subtracted by the sum of the amount of money produced due to the power generated by the solar panel without the Eva system installed and the total cost of the system and water. This total profit equation is listed below as **Equation 6.8**.

$$P = \$cool - (\$nocool + \$manufacturing + \$water) \qquad Equation\ 6.8$$

P stands for total profit. $\$cool$ stands for money made due to power generated by the solar panel with cooling. $\$nocool$ stands for money made due to power generated by the solar panel without cooling. $\$manufacturing$ stands for the total manufacturing costs. $\$water$ represents the total cost of water. The results from the simulation are shown below.

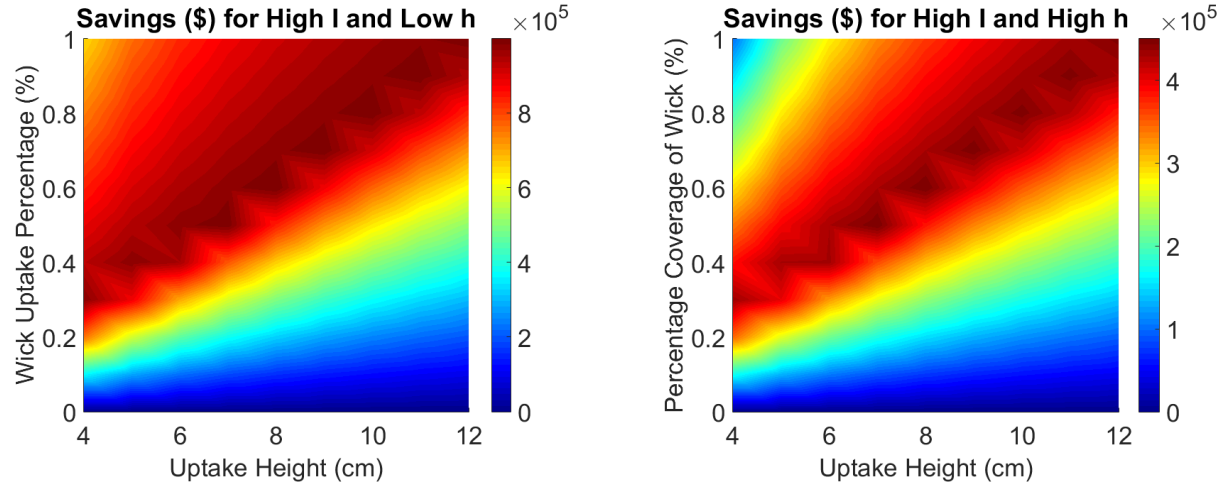

*Figures 6.6: Simulation for **high** incoming solar irradiation with **low** convection coefficient (left) and **high** convection coefficient (right)*

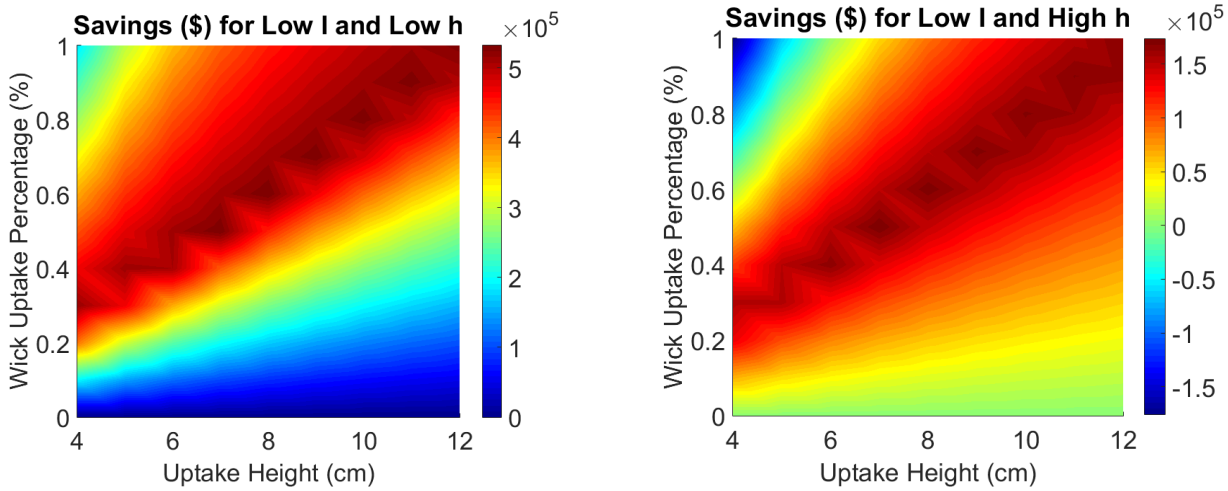

*Figures 6.7: Simulation for **low** incoming solar irradiation with **low** convection coefficient (left) and **high** convection coefficient (right)*

The plots depict the range of wick uptake heights on the x-axis and the wick uptake percent coverages on the y-axis. The colorbar represents the amount of money made or lost with the use of the EVA system. The total profit depicted on the colorbar assumes that this system is fitted onto 10,000 solar panels in a solar farm and operates over a lifetime of 20 years. Four different scenarios were tested based on incoming solar irradiation and heat transfer convection coefficient. The darker red band represents the most profit for the EVA system. Across the four different scenarios tested, the dark red band for the most part overlapped, and so, this region represented the optimal setup for the EVA system.

Transient Model

Based on these results, an optimal wick uptake height and wick uptake percent coverage was selected from the dark red regions in the plots. These results were then inputted into a transient heat model to create a model for general scenarios. This transient model used data from Tallahassee, FL to evaluate the temperature of the solar panel on a given day. Tallahassee, FL was selected as the case study because of its location in the Gulf Coast region of the United States. Our previous research revealed that the places where there was a lot of solar irradiation as well as rainfall in the United States was in the Gulf Coast region. (This data regarding the rainiest and sunniest regions in the United States is attached in the **Appendix**) Hence, the data regarding the ambient temperature and the incoming solar irradiation was used to create the transient heat transfer simulation. This model took this information and inputted it into the transient heat equation. The transient heat equation is shown in **Equation 6.8** where m_{panel} stands for the mass of the solar panel and c_{panel}l stands for the heat capacity of the solar panel.

$$Q_{in} - Q_{out} = m_{panel} c_{panel} (T_{solarpanel} - T_{solarpanel\,initial}) \qquad Equation\ 6.8$$

For each second of the day, $T_{solarpanel}$ was evaluated for two scenarios: 1.) when the solar panel is fitted with the EVA system and 2.) when there is no EVA system retrofitted to the panel. The two scenarios result in the value of of Q_{out} in **Equation 6.8** changing from including the heat loss due to evaporation along with radiation and convection and not including it respectively. The transient rate of evaporation is included in each time step of the model because the rate of evaporation changes based on incoming solar irradiation and temperature of the solar panel.

The temperature of the solar panel with cooling and without cooling is evaluated and plotted for the entire day and the results are shown in **Figure 6.8**. As seen in that figure, the Eva system has a clear reduction in the temperature of the system with a maximum difference at the peak of the solar irradiation at approximately 30℃.

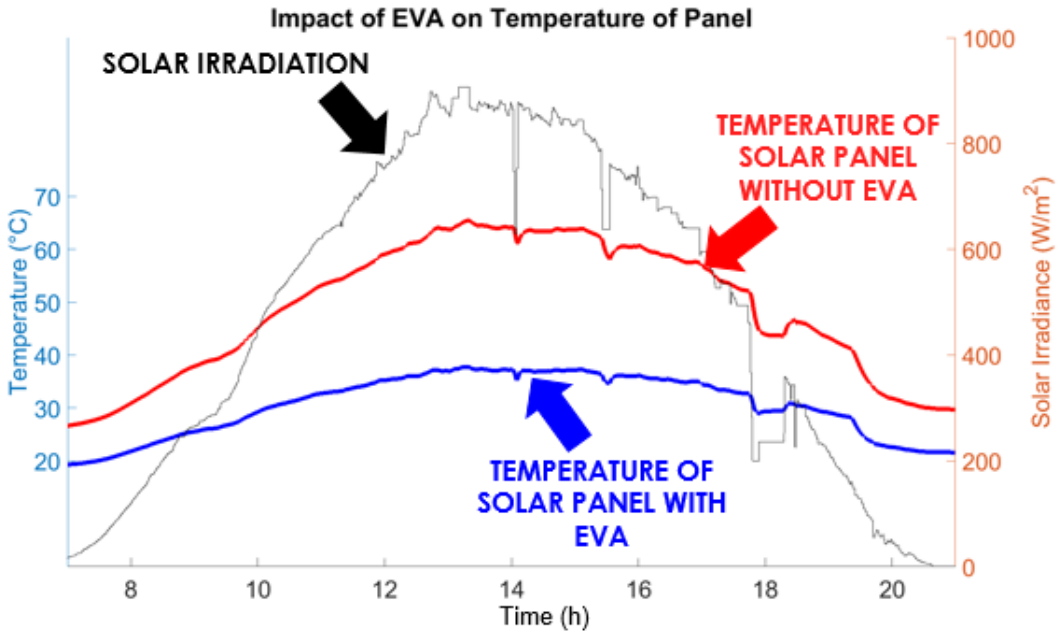

Figure 6.8: The temperature decrease with EVA

In addition to evaluating the temperature of the solar panel, the increased power generated by the solar panel is also evaluated. Similarly to the steady state optimization model described earlier, the ambient temperature throughout the day and the incoming solar irradiation are used to determine the amount of power generated by the solar panel when it is being cooled and when it is not. The results of this evaluation are shown in **Figure 6.9**. As seen in that figure, the Eva system has a clear increase in the power production of the solar panel throughout the day. It was determined that a solar panel with Eva under these conditions for a year will provide savings of **$24/year**.

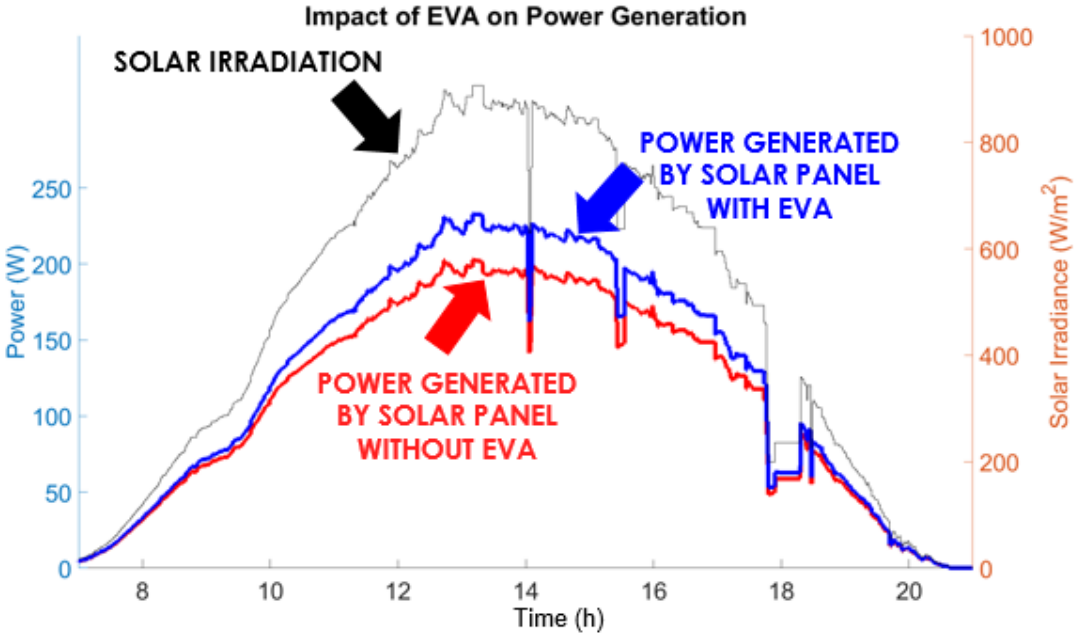

Figure 6.9: The power increase with EVA

This transient model was used to compare the test results from both the indoor and outdoor tests for the small scale and large scale solar panels.

6.3 Indoors Validation Test

Lamp Station

Before indoor testing could be performed, a lamp station needed to be created to hold bulbs that would simulate the solar irradiation indoors. Refer to the Appendix for engineering drawings of the solar panel station and lamp station that were built.

Both stations work with varying angles of the solar panel, in order to obtain any desired angle of incidence for testing indoors. The screws simply have to be placed in one of the several holes available for mounting the lamp station arms that hold the bulbs. The solar panel station allows for varying angles of incidence for testing outdoors. Both stations were made of quarter inch acrylic and laser cut in the RPL. Each bulb operates at 50 W and 12 V with a current of 4.16 A. The bulbs we purchased were GE Constant Color Precise Halogen bulbs with a dichroic reflector, which output a spectrum that imitates that of solar irradiation, as shown in the diagram below.

Figure 6.10: Halogen bulb with dichroic reflector.

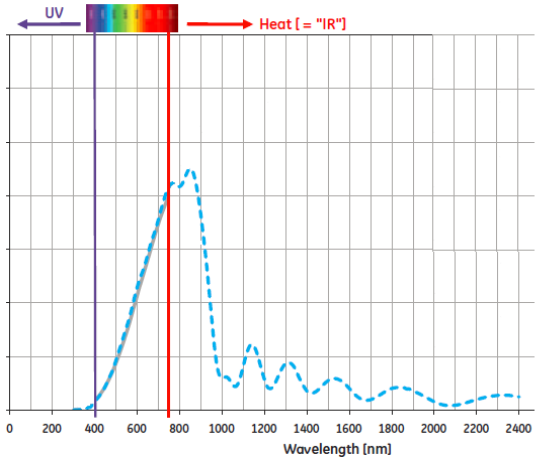

Figure 6.11: Bulb spectrum from GE [19].

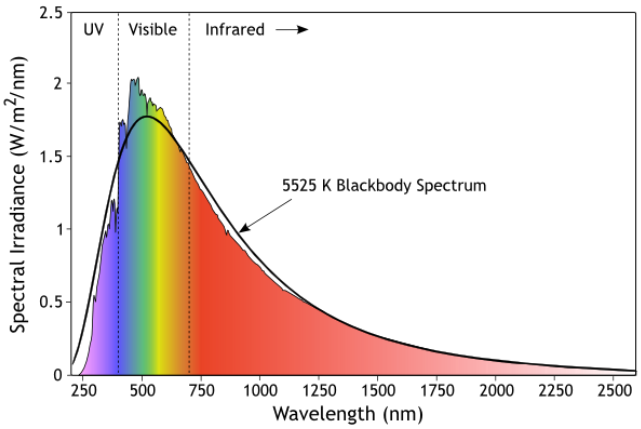

Figure 6.12: Blackbody spectrum of the Sun [20].

The lamps were powered using the power supplies available in the GM lab, with one two-sided power supply able to power 3 bulbs. One side of the power supply powers 2 bulbs with 24 volts and 4 amps, and the other powers one bulb with 12 volts and 4 amps. Precautions were taken to not overpower the bulbs. This station was then utilized for the indoors validation testing.

Due to the cold climate, validation tests which involved the heating-cooling tests performed earlier but this time including lighting for power output measurements. 2 GE halogen 50W lamps with dichroic reflectors were used as they were cost-effective but still produced light closely resembling the solar spectrum.

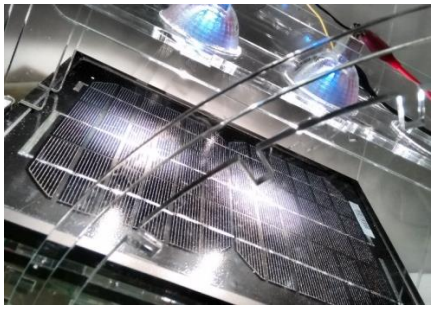

Figure 6.13: Indoors validation test setup.

Figure 6.14: Indoors validation test setup.

As the lamps heat and power output could not be ascertained, the heat sheets were used to heat it initially to the maximum, steady-state temperature before the open circuit voltage, V_{OC} and short circuit current, I_{SC} readings were taken within a minute after the removal of the heating aluminium plate. After that, the heating plate was reinstated on the surface of the solar panel and Eva was used to cool it down to a steady-state temperature before the readings were taken again.

The maximum power output of a solar panel under a given illumination condition is equal to V_{OC} x I_{SC} x FF. FF is the electrical fill factor of the solar panel. The exact FF could not be determined exactly without a variable resistor circuit (made for demo—see Section 7) and time to attain the correct load resistance value. However, it is known that the fill factor of a photovoltaic cell decreases with increasing temperature (Source: Non-Conventional Energy Resources (pg. 128), by B H Khan). Hence, the minimum increase in power output can be determined using the following formula:

$$Min\ \%\ Increase\ in\ Power\ Output = \frac{V_{OC,c} * I_{SC,c} - V_{OC,h} * I_{SC,h}}{V_{OC,h} * I_{SC,h}}$$

where $V_{OC,c}$the open circuit voltage at the minimum temperature with Eva is, $I_{SC,c}$ is the short circuit current at the minimum temperature with Eva, $V_{OC,h}$ is the open circuit voltage at the maximum temperature without Eva, and $I_{SC,h}$ is the short circuit current at the maximum temperature without Eva.

	ΔT [ºC]	Increase in Power Output [%]
Model Predictions	-17	9.0
Experimental Results	-14	>9.6

Table 6.2: Model predictions vs experimental results for indoor testing.

The higher increase in power output could be attributed that temperature has a stronger effect on photovoltaics' efficiency under low lighting conditions.

6.4 Outdoors Validation Test

During the last week of the project, conditions became favorable and outdoor validation tests were conducted for both the small-scale prototype as well as the mid-sized prototype.

Figure 6.15: Small-scale prototype outdoor test setup.

Small-scale Prototype

2 identical setups were placed beside one-another facing the direction of the Sun (Figure 6.15). One had Eva whereas the other one did not have Eva.

The panel temperatures were allowed to reach steady state when the readings were taken at 4.30pm. The direct irradiation at the time was 770W/m^2. Again, the open circuit voltage and short circuit current readings were recorded.

	ΔT [^{o}C]	Increase in Power Output [%]
Model Predictions	-14	6.9
Experimental Results	-12	>5.2

Table 6.3: Model predictions vs experimental results for small-scale outdoor testing.

The reason behind the outdoors validation test over-predicting the power output increase but the indoors validation test under-predicting the power output increase may be due to the efficiency dependence on temperature decreasing at higher illumination levels.

Medium Scale Prototype

Figure 6.16: Medium scale prototype in the field.

For the outdoor tests a medium scale prototype was built, as shown in figure 6.16. To understand the design, construction, and function of this prototype, refer to the section on design. The solar

panel used was a Renogy 100 Watt panel. The fabric used was the Broadcloth fabric cotton-polyester blend. The mesh used was the polypropylene perforated sheet. A frame was built that as installed across the length of the panel on the backside, whose specifications are in the appendix. The frame was held on by bolts that were put through the inner bottom and top holes that are on the frame of the panel.

Figure 6.17: Inside of the Water Containment Unit during the outdoor test.

To get water into the system, a hole was present in the wick containment unit that allowed the observation the float valve. Although float valve was tested by attaching a hose and running water through it, for the purposes of testing the ability for the wicking arrangement the float system wasn't necessary. Water was poured into the observation hole, and a piece of mesh was placed over the hole to block any particulates from entering.

A green colored dye was used in the water with the intention of being able to track the progress of the water as it was wicked through the fabric, but the fabric unexpectedly did not wick the food coloring completely. It showed that the wicking process of water will allow for the water in the WCU to be tinged and dirty, but the wicking process will not allow that to come onto the fabric and potentially build up.

The frame used its job of securing most of the mesh against the back of the panel, but needed to be expanded for future purposes. When the water wicked through the entire length of the fabric, there were sites of sagging, where the fabric was not pressed against the panel.

Ideally, there would have been several tests, using more than one panel to set up a control for the day, alongside measuring power output. Due to time constraints though, one panel was used. Power output was not measured because due to the inability to reliably reproduce the day with its irradiation and wind speeds, so the power reading would not have given much data other than showing what was already known regarding power output and temperature.

The panel was set up first, and it sat in the sun until it reached a steady temperature of about 55°C. This was from about 1200 to 1340. At 1340, water was poured into the WCU, and simply let the wicking take place for the next two hours. There was some dripping from the WCU to the outside of the panel onto the grass, so it was periodically filled it with measured amount of water. Water usage for the outdoor test, taking into account the leak, was 0.25 gallons per hour.

Figure 6.18: Backside of the solar panel during outdoor testing.

Thermocouples (the same used for the smaller scale tests) were placed 30 cm away from the center of the panels' length, to record temperature in two locations.

The temperature results from the test are given in Figure 6.19. The results show that a temperature decrease of above 10°C.

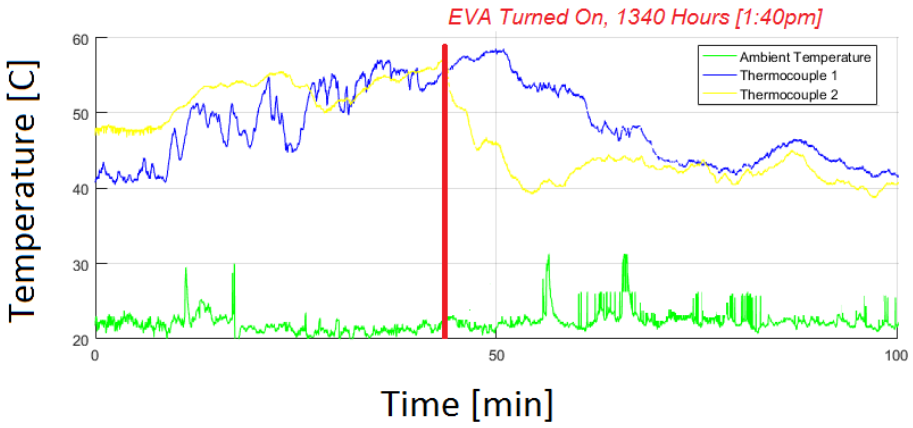

Figure 6.19: Temperature results from outdoor testing.

6.5 Demonstration Setup

A demonstration was created to show the live performance increase of solar panels through the use of the EVA system.

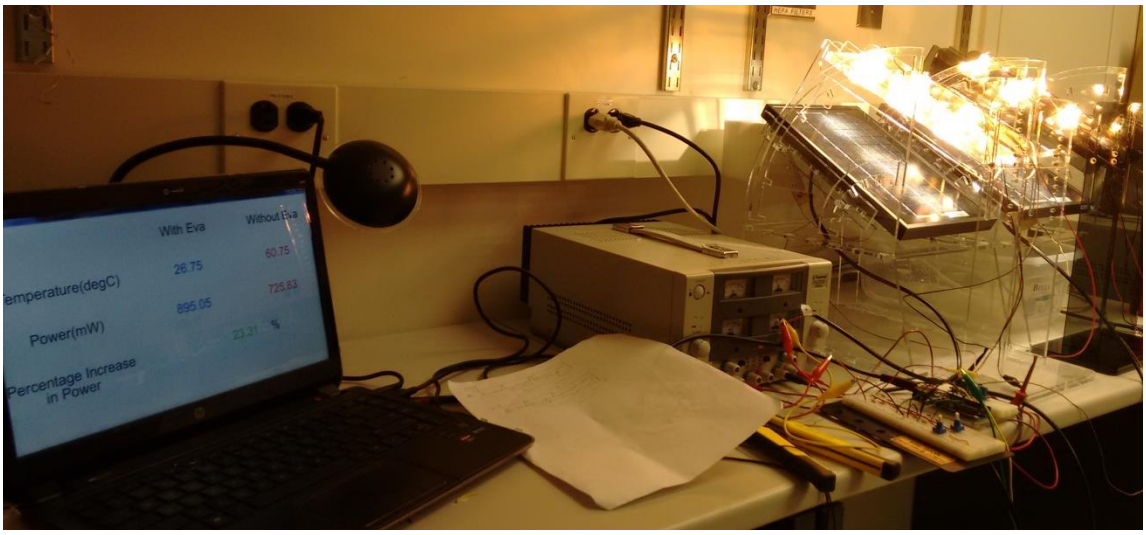

Figure 6.20: Overview of the demonstration setup.

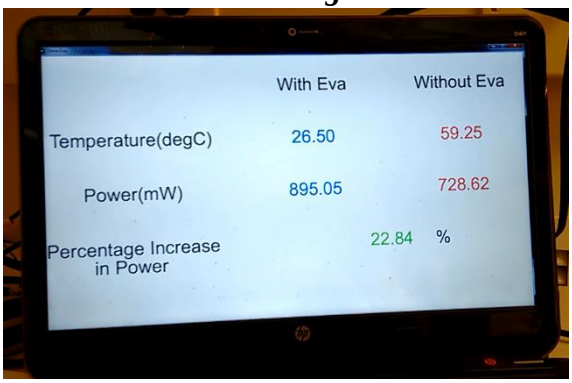

Figure 6.21: Live display of important values.

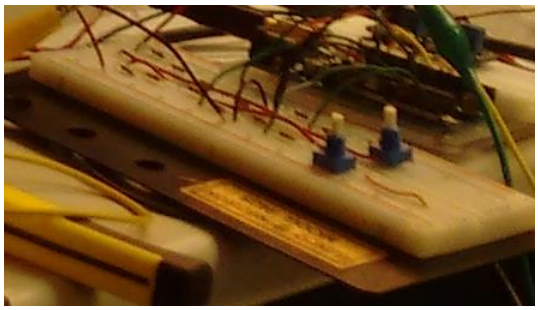

Figure 6.22: Variable resistor circuit.

This live demonstration on the increase of power output from using Eva was created with a variable resistor circuit (see right) that allows for manual adjustment of the load resistance to get the maximum power output. Two setups with the same heating and lighting elements (halogen lamps) and the same solar panels were used. The only difference between the two setups was one of them had the Eva system whereas the other one did not have it. The variable resistor circuit consisted of 4 voltage dividers, 2 for each setup. An Arduino Uno read voltage values from the variable resistor circuit, output the total power output and calculated the percentage increase in power output. Temperature readings were also taken using thermocouples through the same Arduino microcontroller. These live readings were then displayed on a computer screen. The reason for 2 voltage dividers for each setup was that the Arduino Uno could only measure up to 5.5V, whereas the solar panels' maximum power point occurred at voltages of ~8V. Therefore, the voltage was split about evenly across the 2 voltage dividers, where the resistor values were carefully selected to accommodate a potentiometer for selecting the maximum power point with changing temperatures.

SECTION 7:
DISCUSSION

Target versus Accomplished Performance

At the end of this year, the target of creating a fully passive cooling system was achieved. Many options related to methods of cooling were considered; however, after evaluating the advantages and disadvantages of each system, passive cooling came to be the most cost effective, simple and reliable cooling method. The EvaporaSun system only uses cotton, water and a float valve as the main components of its operation. In the end, both the small scale and the larger scale system that were created only utilized this passive technology to cool the solar panels.

The system built not only met but exceeded the basic, intermediate and reach goals set in the beginning of the project. The Eva system increases electrical power output by an average of 10%. It is also fully passive system, using no electrical power, meeting the <0.155kWh/day requirement and net electrical power increase. However, there still is energy usage in the form of embodied energy in the water supply, which is taken into account when calculating the operating cost of the system. From simulations on a solar panel installed in Tallahassee, Florida, the Eva system will provide savings of up to $24 per year. Considering the cost of the full scale system is projected to be $46 per panel, the breakeven point is within 2 years. This satisfied both the intermediate goals of the project. Finally, the prototype was retrofitted onto an average solar panel that has fixtures similar to the ones used on solar farms, proving that the Eva system can be attached to existing solar panels on solar farms. From start to finish, the installation took less than 30 minutes, exceeding the 1 hour installation reach goal. The Eva system had a modular design. However due to resource constraints, it could not be tested with a second solar panel. In addition, the goal of designing, evaluating through experimentation, simulating and testing the design by the end of the year was met.

The main method of cooling is through wicking. All the testing and validation were done using a ribbed cotton material. However, for the sake of durability over the lifetime of the solar panel, it would be better to use a material with a polyester blend. Because the wicking rate is much slower, it was difficult to run multiple tests with this material and so the team chose to use the ribbed cotton material for all the validation tests. In the end, extensive analysis on the effectiveness the polyester blend will have on the cooling of the solar panel was not done and so testing the durability of the overall EVA system was not accomplished.

Lessons Learned

Water is a precious resource and it is important to use as little of it as possible. In our world today, where there is plenty of resources to generate electricity but not enough water available to serve all the people in our world today, water conservation plays a more important role than increasing energy production. Many people still do not have access to clean water for drinking or cooking, and the claim of supplying municipal water to the EVA system will deter many organizations from choosing to use the system because of the amount of water it consumes.

In addition, the source of where this water would come from often proved to be contentious. Since a lot of water is needed to run this system, rainwater alone cannot be used. However, it

would be possible to build an additional large storage tank to collect rainwater and supply it to the WCU along with the municipal supply. This would mean that to maximize the benefit of using rainwater, the EVA system needs to be deployed in areas where there is a lot of sunshine and a lot of rain at the same time. This scenario limits the places where the EVA system could be used. Because of this limited scope, the team chose to use municipal water to provide the water for wicking to have an expanded market that this technology could be used in.

In addition, it would have been practical to provide some kind of visual impact relating to the increase in power output the EVA system will provide solar panels with. This would provide those examining our project to grasp the impact of these percent increase in power performance. For example, by showing how many solar panels less could be installed merely through the use of this system as the increase in power output will be equivalent to many solar panels, then there would be a more concrete understanding of the overall impact of the EVA system.

Recommendations

One of the main recommendations is to invite solar panel manufacturers to consider building the EVA system onto new solar panels that are being constructed. Making the EVA system naturally part of the design of solar panels would minimize any losses from retrofitting the system.

The other recommendation is to perform further outdoor tests using another identical medium size solar panel that will act as a control. A Maximum Power Point Tracker will be used which will automatically determine the maximum power output of the system. This way, the temperature and power data can be simultaneously measured.

Further testing can be done on other materials to be used as wick fabric. It is known that there are certain polyester fabric that perform better than cotton and this could lead to more durable wick fabric.

Optimizing the design of the WCU will also be necessary, since that was rather large for our purposes. That would require an even smaller float valve, but with more resources, a smaller float valve and WCU could be integrated together. This would diminish the already low material costs for Eva, making it more profitable.

Creating a more elegant frame for the back of the panel is also recommended, to stop the possible sagging and drip spots that were observed during the medium scale tests.

A final recommendation is to design a system that will integrate in the structure of the solar panel. This will invite solar panel manufacturers to consider building the EVA system onto new solar panels that are being constructed. Making the EVA system naturally part of the design of solar panels would minimize any losses from retrofitting the system.

SECTION 8:

BUDGET, DONATIONS and RESOURCES

8.1 Budget

Category	Details	Budget	Spent	Balance
Experiments	**Experiments to Validate Simulations**	**$600**	**$485**	**$115**
Evaporation Rate	Lights, acrylic, heats strips	$200	$246	($46)
Cooling Methods	Piping, aluminum, insulation, MDF	$200	$204	($4)
Wicking Rates	Cotton, polyester	$100	$35	$65
Electronics	**Sensors & other tools to measure data**	**$300**	**$274**	**$26**
Thermocouples	Thermocouples with amplifiers	$150	$214	($64)
Misc. Measuremet tools	Flowmeter, anenonmeter, etc.	$150	$60	$90
Medium Scale EVA System	**System to test in outdoor conditions**	**$300**	**$291**	**$9**
Framing & Support	Material to support components	$150	$204	($54)
Water Containment & Transport	Pipes, cotton, and valve for water	$150	$87	$63
Prototyping	**Small scale testing of EVA functionality**	**$200**	**$158**	**$42**
Small Scale EVA	3D printing, acrylic	$150	$120	$30
Water Collector	Rubber, tubes, brackets	$50	$38	$12
Solar Panel	**100 W Solar Panel**	**$200**	**$140**	**$60**
Total		**$1,600**	**$1,348**	**$252**

During the fall semester, only $400 was utilized which was allocated for the cooling method experiments performed to determine a cooling method that had the highest potential for cost savings in a solar farm.

SECTION 9:

REFERENCES

[1] Climatecentral.org, 'MIT: ‘Massive’ Solar Expansion Critical for Climate', 2015. [Online]. Available: http://www.climatecentral.org/news/solar-expansion-critical-for-climate-mit-18973. [Accessed: 02- May- 2016].

[2] Solartown.com, 'Cooling Solar Panels to Increase Efficiency | SolarTown Blog « SolarTown Blog', 2015. [Online]. Available: https://www.solartown.com/blog/2014/09/cooling-solar-panels-to-increase-efficiency/. [Accessed: 02- May- 2016].

[3] Entegrag.com ‘Integra Global’, 2015 [Online] Available: http://www.integrag.com/eng/cleanandcool/sub10.php. [Accessed: 02-May-2016]

[4] Ecoppia.com, ‘Eccopia - Robotic Solar Cleaning Solution’ 2015 [Online]

Available: http://www.ecoppia.com/ [Accessed: 02 - May - 2016]

[5] Economist.com, “Daily Chart: Pricing Sunshine’ 2012 [Online]

Available: http://www.economist.com/blogs/graphicdetail/2012/12/daily-chart-19 [Accessed: 02 - May - 2016]

[6] IM72 Series Photovoltaic Modules: Peak Power: 285 - 295Wp, 1st ed. Moltech, 2012.

[7] Solar-facts-and-advice.com, 'Solar Panel Temperature – Facts and Tips', 2015. [Online]. Available: http://www.solar-facts-and-advice.com/solar-panel-temperature.html. [Accessed: 03- Nov- 2015].

[8] S. Wu and C. Xiong, 'Passive Cooling Technology for Photovoltaic Panels for Domestic Houses', International Journal of Low-Carbon Technologies, vol. 0, pp. 1-9, 2014.

[9] Integrag.com, 'Integra Global', 2015. [Online]. Available: http://www.integrag.com/eng/. [Accessed: 02- May- 2016].

[10] Cleantechnica.com, ‘Average Electricity Prices Around the World’, 2013 [Online].

Available: http://cleantechnica.com/2013/09/30/average-electricity-prices-around-world/ [Accessed 02-May-2016]

[11] LATimes.com, ‘U.S. Electricity Prices May Be Going Up For Good’, 2014 [Online].

Available: http://www.latimes.com/nation/la-na-power-prices-20140426-story.html [Accessed: 02-May-2016]

[12] S. Wu and C. Xiong, 'Passive Cooling Technology for Photovoltaic Panels for Domestic Houses', *International Journal of Low-Carbon Technologies*, vol. 0, pp. 1-9, 2014.

[13] A. Jones and C. Underwood, 'A Thermal Model for Photovoltaic Systems', *Solar Energy*, vol. 70, no. 4, pp. 349-359, 2001.

[14] Motech, *IM72 Series Photovoltaic Modules: Peak Power: 285 - 295Wp,* A version. Motech Industries Solar Division, 2012.

[15] Engineersedge.com, 'Convective Heat Transfer Coefficients Table Chart | Engineers Edge | www.engineersedge.com', 2015. [Online]. Available: http://www.engineersedge.com/heat_transfer/convective_heat_transfer_coefficients__13378.htm . [Accessed: 04- Nov- 2015].

[16] H. Bahaidarah, A. Subhan, P. Gandhidasan and S. Rehman, "Performance evaluation of a PV (photovoltaic) module by back surface water cooling for hot climatic conditions", Energy, vol. 59, pp. 445-453, 2013.

[17] Y. Irwan, W. Leow, M. Irwanto, Fareq.M, A. Amelia, N. Gomesh and I. Safwati, "Indoor Test Performance of PV Panel through Water Cooling Method", Energy Procedia, vol. 79, pp. 604-611, 2015.

[18] A. Baloch, H. Bahaidarah, P. Gandhidasan and F. Al-Sulaiman, "Experimental and numerical performance analysis of a converging channel

[19] GE Lighting, “Constant Color Precise IR,” 99633 Datasheet, Feb. 2010

[20] http://qdl.scs-inc.us/, “Radiation”, 2015 [Online]. Available: http://qdl.scs-inc.us/2ndParty/Pages/10522.html [Accessed: 02-May-2016]

[21] B. Khan, Non-conventional energy resources. New Delhi: Tata McGraw-Hill., 2009.

[22] Amy Le. (2011). Liquid-Level Monitoring Using a Pressure Sensor [Online]. Available:http://www.ti.com.cn/cn/lit/an/snaa127/snaa127.pdf [Accessed: 10-February-2016].

[23] Kevin Hambrice and Henry Hopper (2004, December 1). Leak/Level: A Dozen Ways to Measure Fluid Level and How They Work [Online]. Available: http://www.sensorsmag.com/sensors/leak-level/a-dozen-ways-measure-fluid-level-and-how-they-work-1067 [Accessed: 10-February-2016].

[24] REUK.co.uk (2014, September 24). Float Switch Water Level Measurement [Online]. Available: http://www.reuk.co.uk/Float-Switch-Water-Level-Measurement.htm [Accessed: 10-February-2016].

[25] Mike Shorts. Understand Check Valves: Sizing For The Application, Not The Line Size [Online]. Available: http://www.waterworld.com/articles/print/volume-23/issue-5/editorial-feature/understanding-check-valves-sizing-for-the-application-not-the-line-size.html [Accessed: 10-February-2016].

SECTION 9:

REFERENCES
APPENDIX

Rainfall and Sunshine

City	Amount of Rain (inches)	Number of Rainy Days
Mobile, Alabama	**67**	**59**
Pensacola, Florida	**65**	**56**
New Orleans, Louisiana	**64**	**56**
West Palm Beach, Florida	**63**	**58**
Lafayette, Louisiana	**62**	**55**
Baton Rouge, Louisiana	**62**	**56**
Miami, Florida	**62**	**57**
Port Arthur, Texas	**61**	**51**
Tallahassee, Florida	**61**	**56**

Lake Charles, Louisiana	**58**	**50**

Table A: Rainiest Cities in the United States

City	Annual % Avg Possible Sunshine	Annual Insolation (kWh/m^2)
Yuma, Arizona	**90**	**2251**
Redding, California	**88**	**2001**
Las Vegas, Nevada	**85**	**2356**
Phoenix, Arizona	**85**	**2390**
Tucson, Arizona	**85**	**2345**
El Paso, Texas	**84**	**2339**
Fresno, California	**79**	**2104**
Reno, Nevada	**79**	**2152**
Flagstaff, Arizona	**78**	**2202**

Sacramento, California	**78**	**2050**

Table B: Sunniest Cities in the United States

Cites	Annual % Avg Possible Sunshine	Annual Insolation (kWh/m^2)	Annual Rainfall (inches)
Lake Charles, Louisiana	**72**	**1801**	**58**
Miami, Florida	**70**	**1890**	**62**
Pensacola, Florida	**60**	**1784**	**65**
Port Arthur, Texas	**58**	**1788**	**61**
New Orleans, Louisiana	**57**	**1780**	**64**

Table C: Cities with a lot of rain and a lot of sun

Small Scale Prototype Engineering Drawing (PDF version attached)

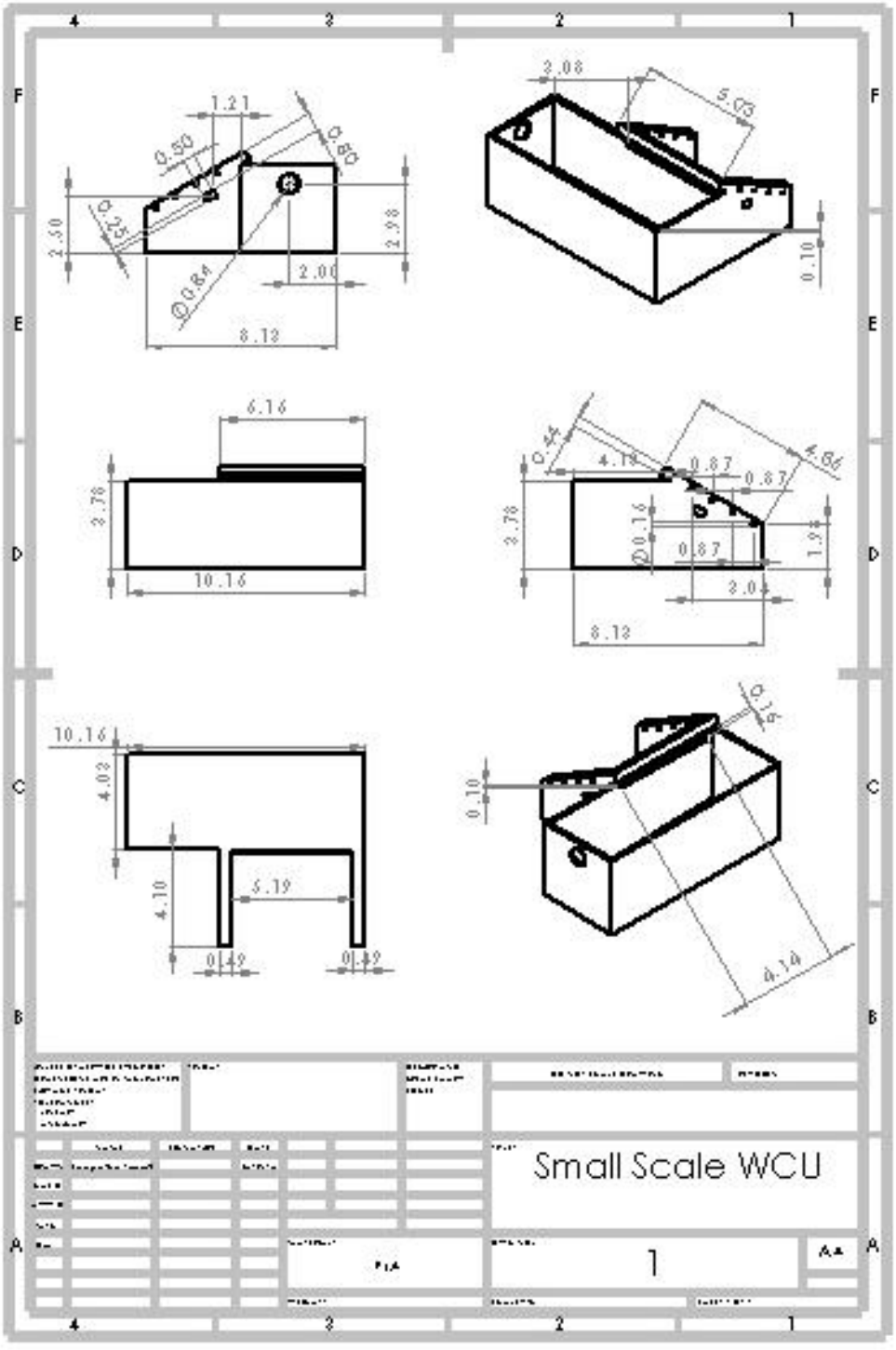

Figure A: Water Containment Unit's engineering drawing.

Heat Fin Equations and Results

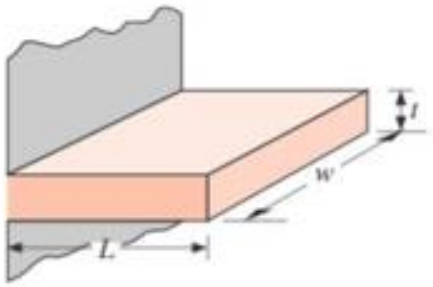

Assumption: Convective Cooling at Tip

$$m = \sqrt{\frac{h * Perimeter_{fin}}{k * A_{fin}}}$$

$$\eta_{fin} = \frac{\tanh(m * L_c)}{m * L_c}$$

$$Rectangular: L_c = L + \left(\frac{t}{2}\right)$$

$$Q_{total_{fin}} = \eta_{total} * h * A_{total} * (T - T_{base})$$

$$\eta_{total} = [1 - \frac{(N * A_f)}{A_{total}} * (1 - \eta_{fin})]$$

$$A_{fin} = w * t$$

$$A_{total} = N(w * t) + A_{base}, N = Number\ of\ Fins$$

Results

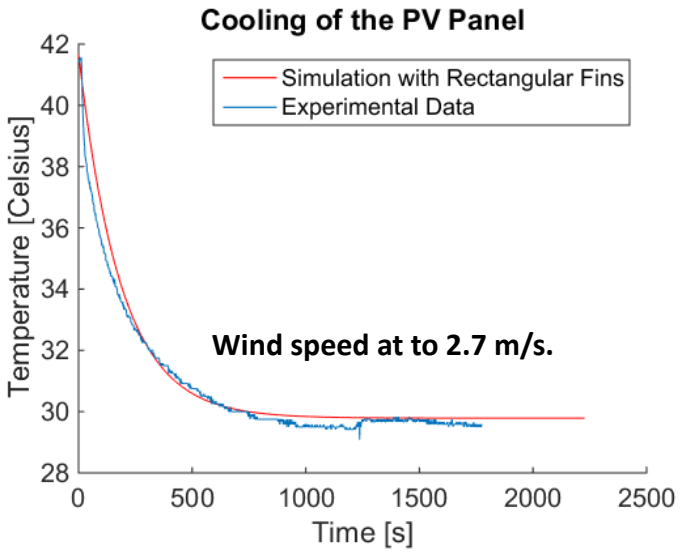

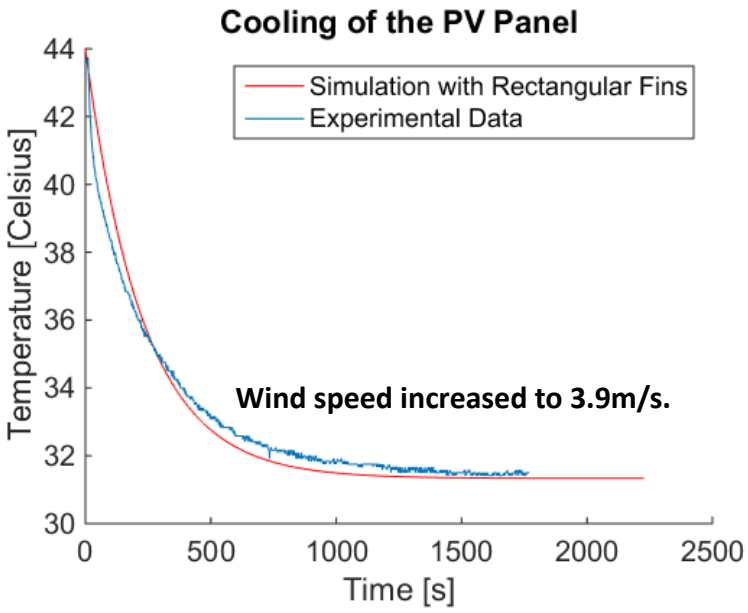

Figures B: Heat fin cooling test results.

Water Transmission Design Choice

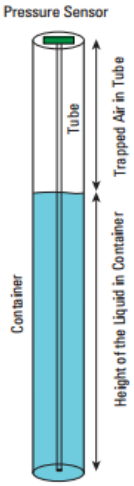

Pressure Sensor [22]

A pressure sensor is used to detect the height of the water. The sensor is consists of an open ended tube and is submerged in the container with water. The amount of water in the container exerts a pressure on the sensor through the trapped air and the sensor outputs this pressure as an equivalent voltage. The problem that is important to deal with is calibration. These sensors need to be calibrated properly before use.

Load Cell [23]

A load cell needs to be placed on the exterior of the container containing the water. It measures the strain changes to evaluate the weight of the water. The main issue with load cells is that it needs to be properly mounted to get accurate measurements.

Ultrasonic Sensor [23]

The ultrasonic sensor is placed on top of a closed container containing the water to measure changes in the water level. The main issues with this sensor are that the range of the sensor is limited and the senor needs to be water proofed in order to not stop working early.

Float Valve [23]

The float ball is connected to the pipe that supplies water and as the float moves up and down it opens and closes the pipe entrance reacting to the changing water level in the container. The main issues are that it consists of moving parts and so it must be examined regularly to make sure that it is operating correctly at all times and there should be no backflow with pressure changes within the container.

Float Switch [24]

A reed float switch consists of a small float mounted on a magnet to sense changing water levels. Depending on where the storage for the water is, it might need the use of a pump. In addition, to operate the reed switches it must be powered by some external source.

Check Valve [25]

A check valve allows for the continuous flow of water without the use of a control system by only using pressures to create the flow. A check valve allows flow only in one direction and so can prevent any backflow. The main issue regarding the check valve is that it can create an overflow of water into the container and so it must be used in conjunction with another control mechanism.

Flow Charts

Overview

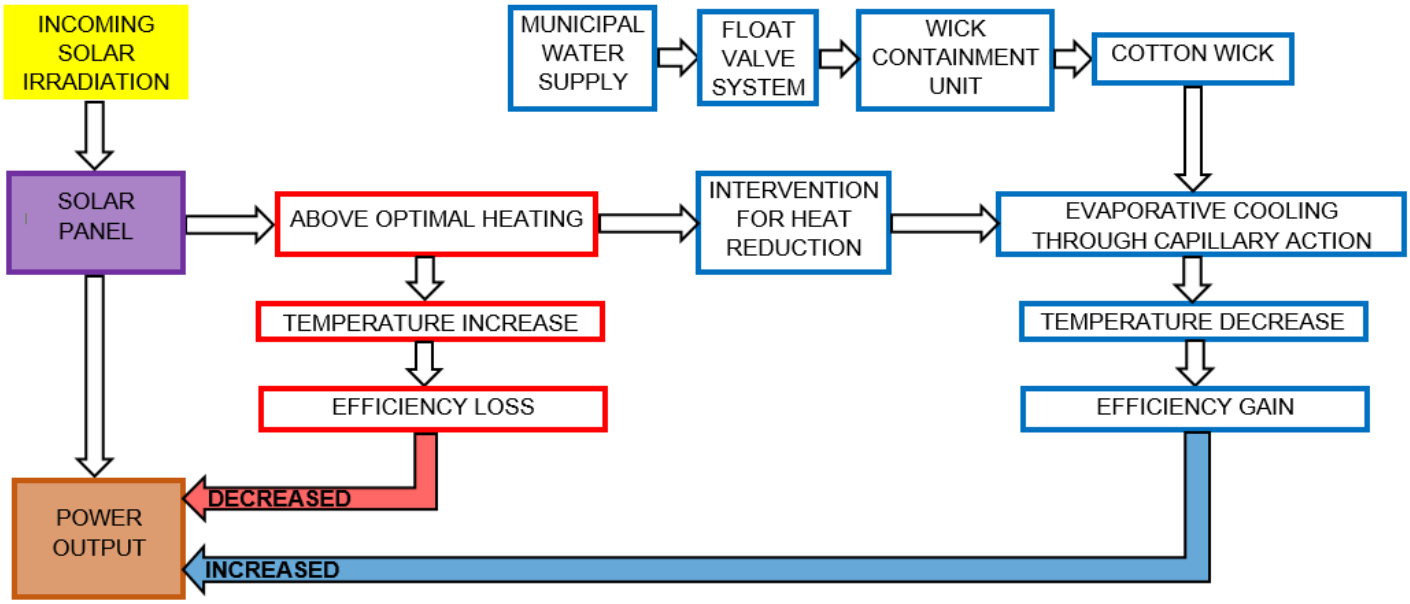

Figure C: System flow chart.

Simulation

Flowchart for calculating the amount of water needed to run EVA.

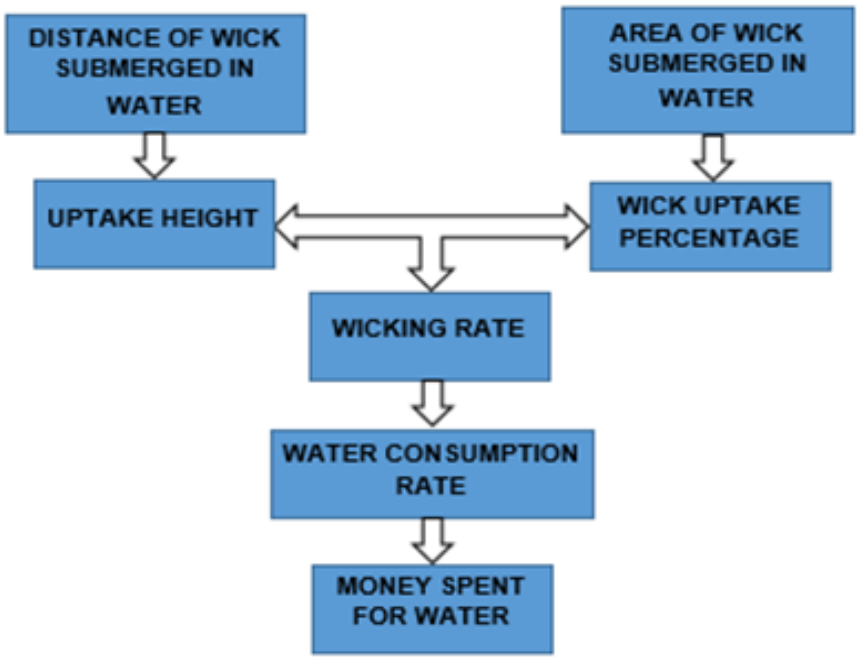

Figure D: Simulation flow chart.

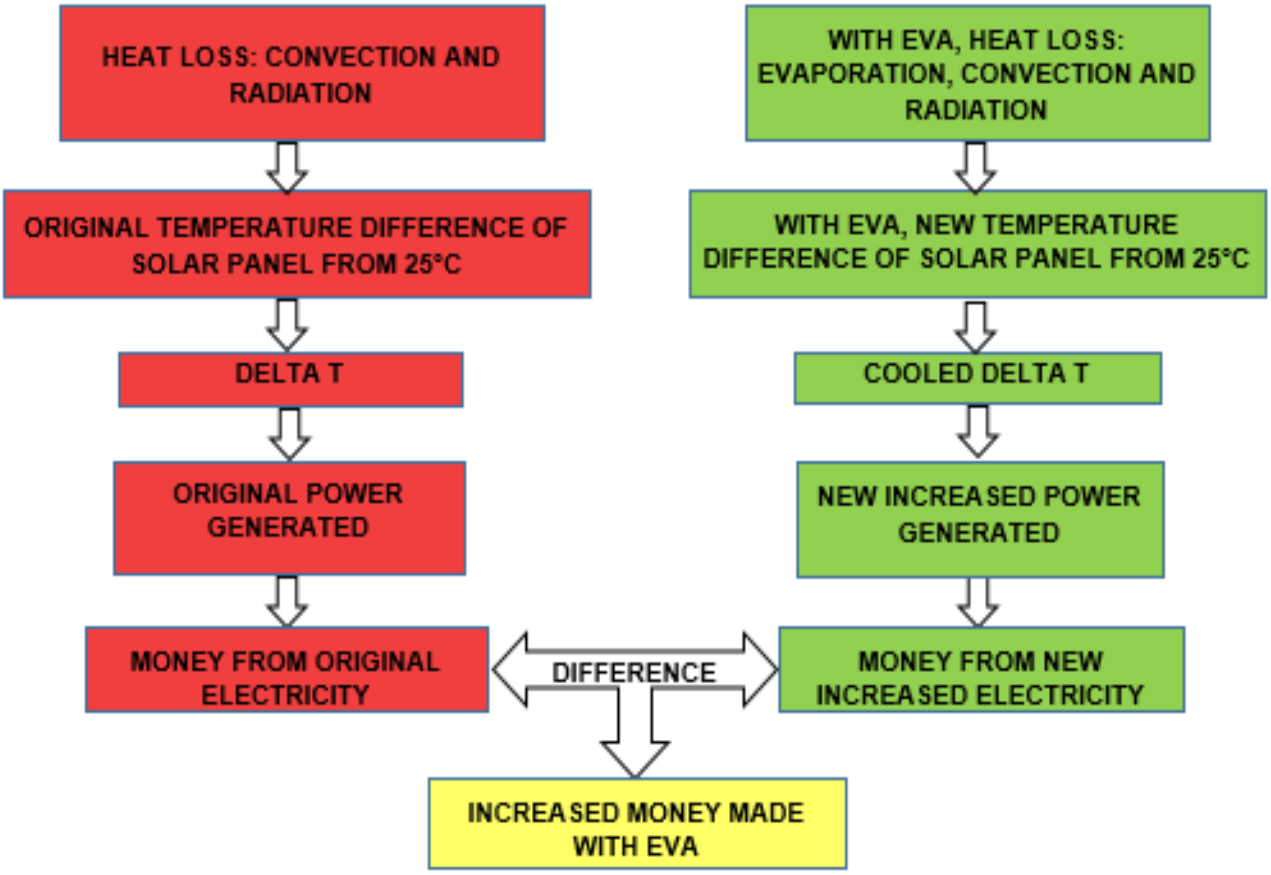

Figure E: Flowchart for the amount of money made from cooling the solar panel with Eva

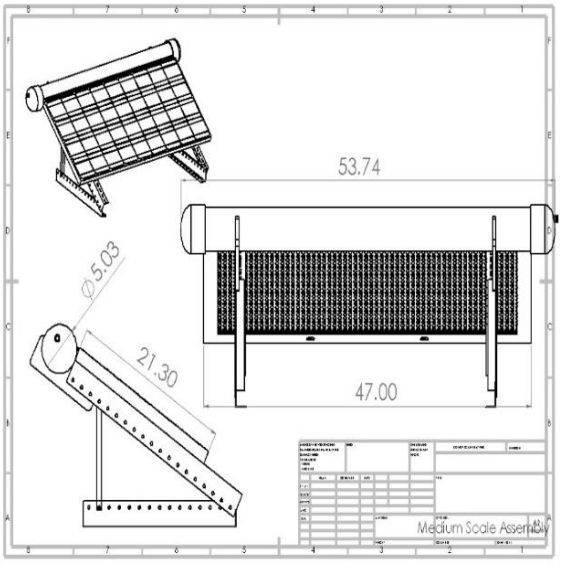

Figure F: Specifications for the entire model and solar panel.

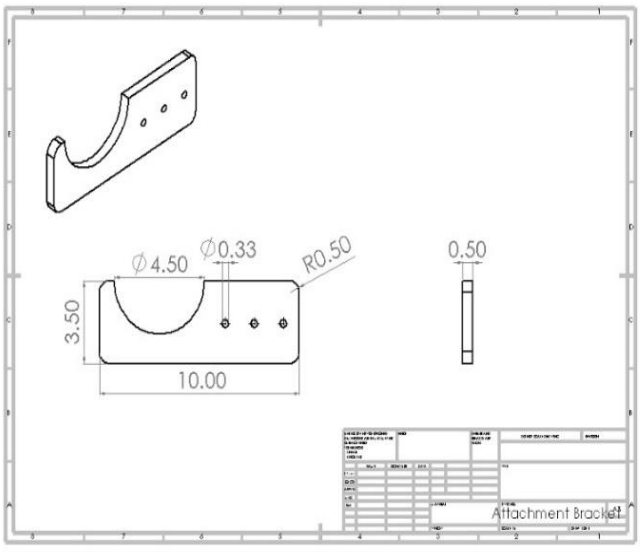

Figure G: Additional mounting material for the attachment of the pipe

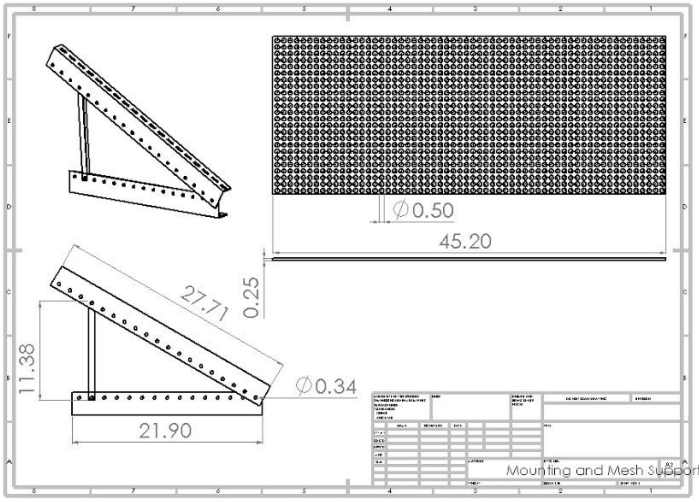

Figure H: Solar panel and Mounting Specifications.

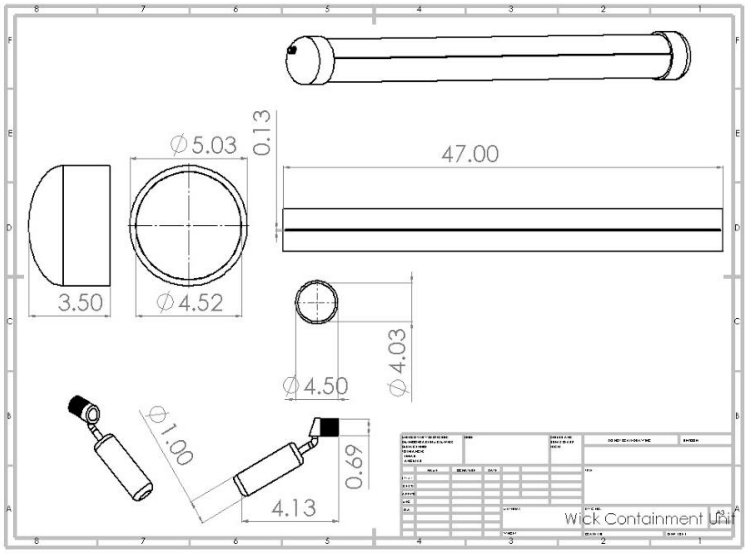

Figure I: Float valve and WCU Specifications.

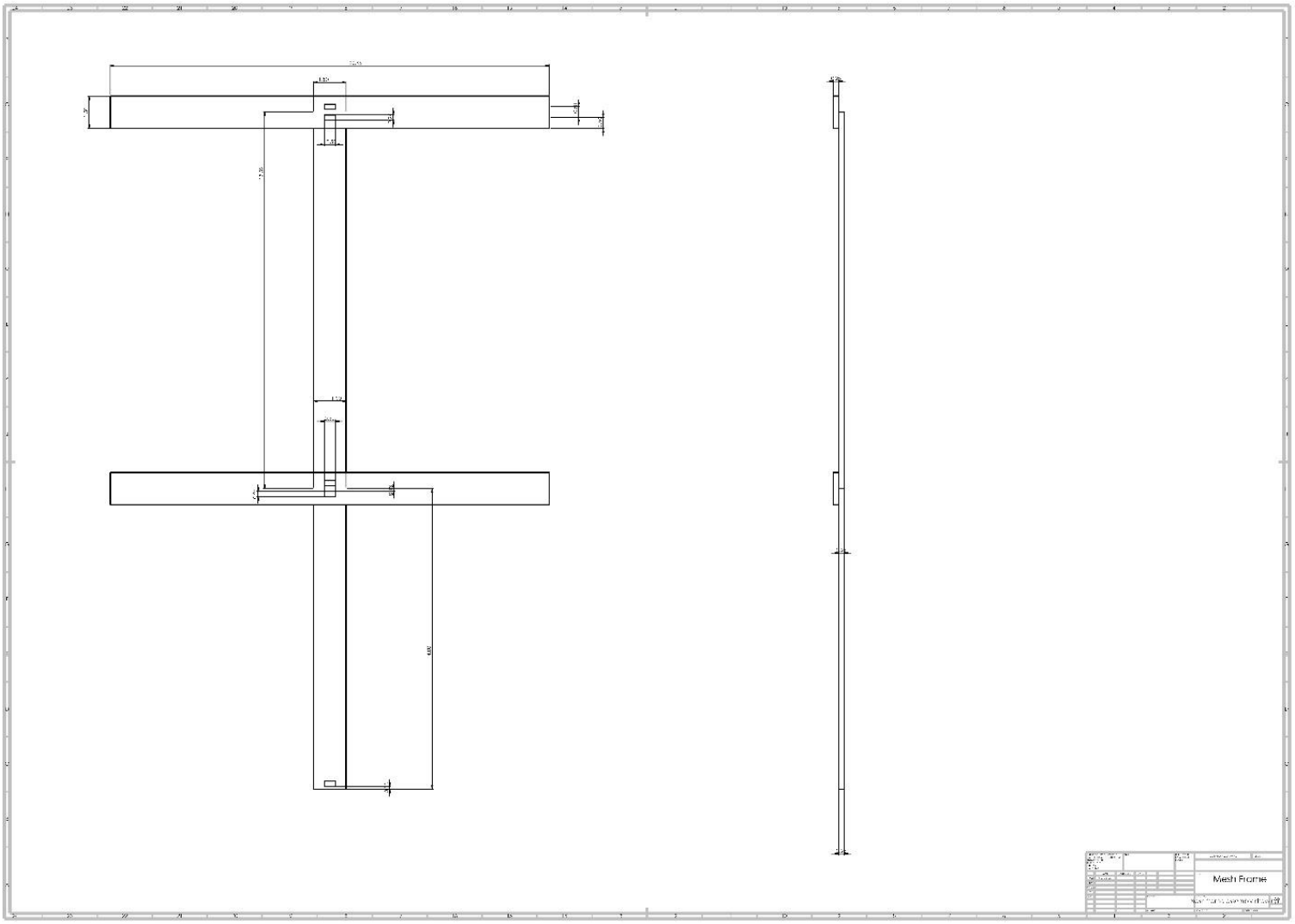

Figure J: Medium Scale Mesh Frame, used to keep mesh and fabric flesh against panel.

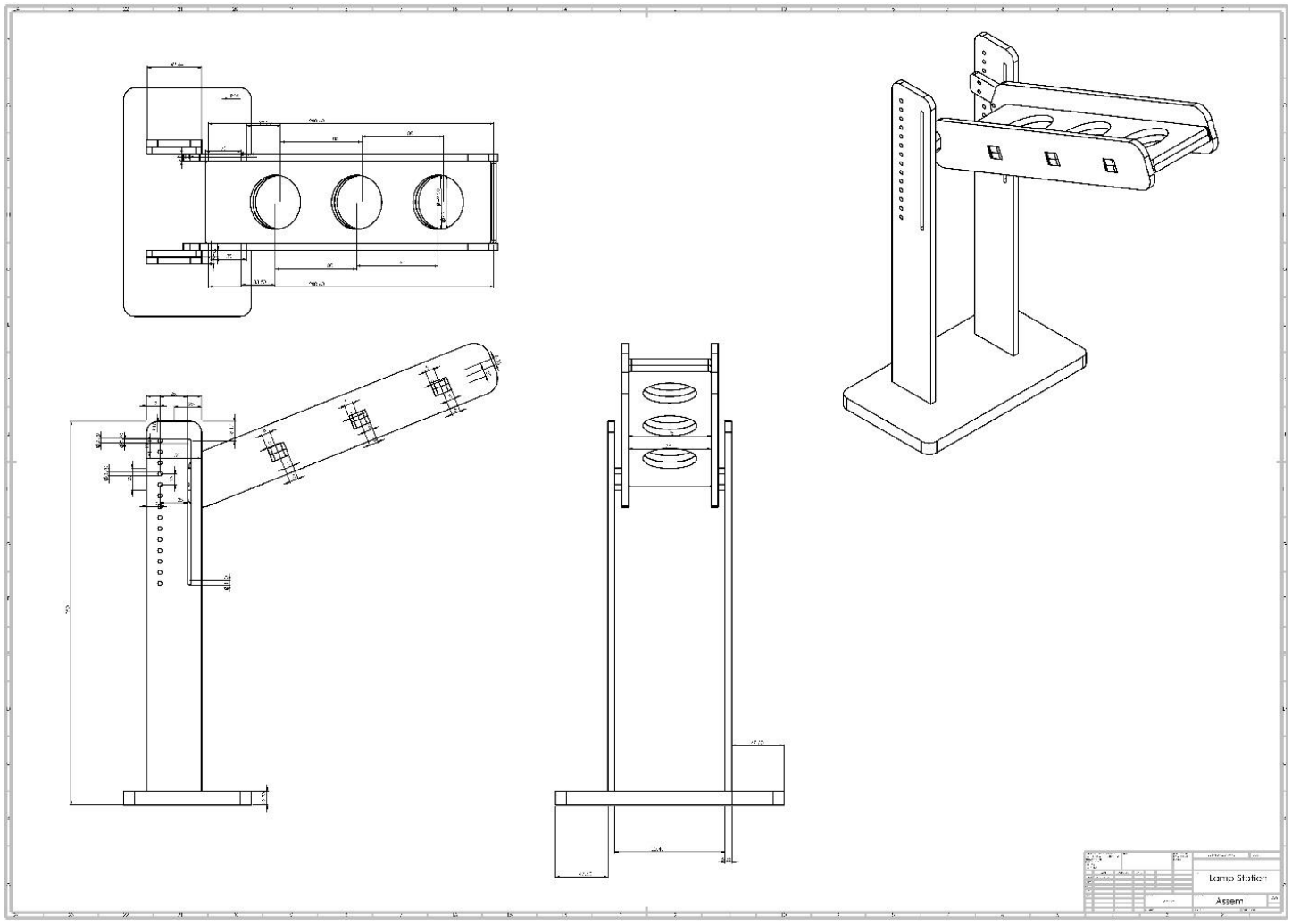

Figure K: Small Scale Solar Panel Lamp Station

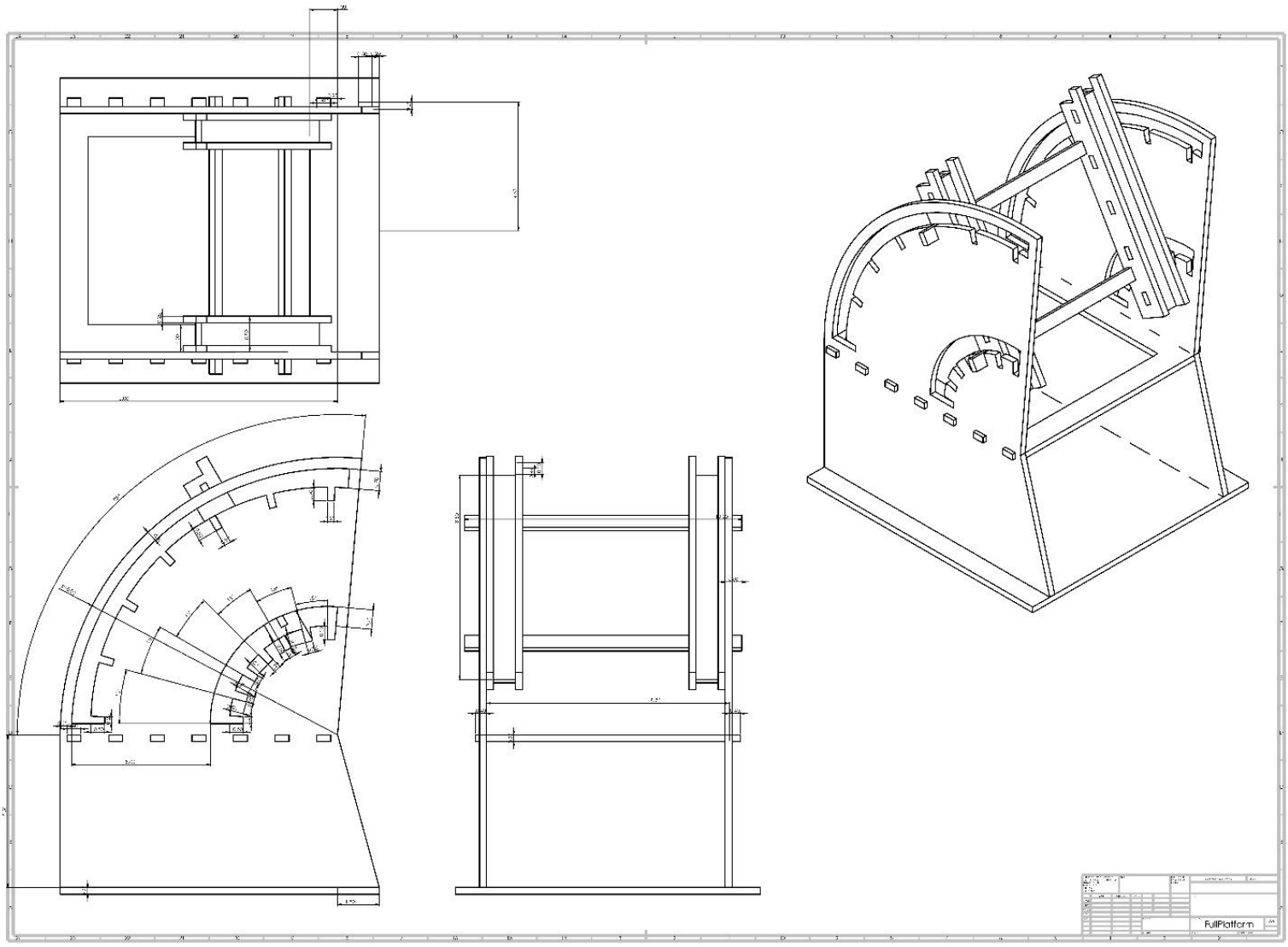

Figure L: Small Scale Solar panel mounting station.